Design and Modeling of OffShore Nuclear Platform Fuel and Transfer System

by

Asia Allison

B.S. Mathematics, Spelman College, 2014

Submitted to the Department of Mechanical Engineering
in partial fulfillment of the requirements for the degrees of

NAVAL ENGINEERS DEGREE

and

MASTERS OF SCIENCE IN MECHANICAL ENGINEERING

at the

MASSACHUSETTS INSTITUTE OF TECHNOLOGY

May 2024

Authored by:	Asia Allison Department of Mechanical Engineering May 10, 2024
Certified by:	Michael Golay Professor of Nuclear Science and Engineering, Thesis Supervisor
Certified by:	Jacopo Buongiorno Professor of Nuclear Science and Engineering, Thesis Reader
Accepted by:	Nicolas Hadjiconstantinou Professor Graduate Officer, Department of Mechanical Engineering

Design and Modeling of OffShore Nuclear Platform Fuel and Transfer System

by

Asia Allison

Submitted to the Department of Mechanical Engineering
on May 10, 2024 in partial fulfillment of the requirements for the degrees of

NAVAL ENGINEERS DEGREE

and

MASTERS OF SCIENCE IN MECHANICAL ENGINEERING

ABSTRACT

The design and modeling of the fuel and transfer system aboard the Offshore Nuclear Platform (OFNP) aims to integrate Small Modular Reactors (SMRs) into an offshore setting. This endeavor is in line with global initiatives to mitigate temperature rise by 2050, using nuclear energy for electrical generation [1] A specific focus on high-temperature gas reactors, notably pebble bed reactors for their compact fuel form and capability for at-power fuel replenishment through TRISO fuel pebbles recirculation will be evaluated. This study will review both historical and current high-temperature gas reactors, focusing on their development, application, and operational efficiencies. Special emphasis will be placed on methods for managing spent fuel, including storage and environmental considerations. The research will develop the platform's conceptual fuel transfer system which details the design of fuel storage, handling and at sea transfer system, ensuring safety, particularly during at-sea offloading operations. Additionally, the thesis will assess the platform's stability, transfer system structural integrity, and shielding design to determine its feasibility for offshore energy generation for the reactor's lifetime.

Thesis supervisor: Michael Golay
Title: Professor of Nuclear Science and Engineering

[1] Text from United Nation Framework Convention on Climate Change: doi:https://unfccc.int/most-requested/key-aspects-of-the-paris-agreement.

Acknowledgments

I would like to show my deepest gratitude to my thesis supervisor, Professor Michael Golay and thesis reader, Professor Jacopo Buongirono, for their guidance throughout this year-long endeavor. They provided me with the support and resources I needed, and the confidence to navigate through the difficult portions of the process.

Finally, I would like to thank my family and friends for their unconditional support and encouragement not only during my two years here in Cambridge but throughout my entire life.

List of Acronyms

CG Center of Gravity

DWT Deadweight Tonnage

FHS Fuel Handling System

FPSO Floating Platform Storage Offloading

GCR Gas Cooled Reactor

GM Transverse Metacentric Height due to Gravity

GZ Righting Arm

HTGR High Temperature Gas Reactor

HVT Half Value Thickness

IMO International Maritime Organization

LCG Longitudianl Center of Gravity

LWR Light Water Reactor

MAXSURF Marine Vessel Analysis And Design Software

MIT Massachusetts Institute of Technology

MWe Megawatt Electric

OFNP Offshore Nuclear Platform

PBR Pebble Bed Reactor

PWR Pressurized Water Reactor

SMR Small Modular Reactor

STS Ship to Ship

SWL Safe Working Load

TCG Transverse Center of Gravity

TRISO Tri-Structural Isotropic

UCO Uranium OxyCarbide

ULCC Ultra Large Crude Carrier

VCG Vertical Center of Gravity

VLCC Very Large Crude Carrier

Contents

List of Figures

List of Tables

Chapter 1

Introduction

1.1 Background

Limiting the rise in global temperatures to no more than 1.5 degree Celsius above pre-industrial levels by the year 2050 has the become the goal for many countries around the world [1]. This ambition, driven by concerns over the detrimental impacts of climate change, may lead to a transformation in the way we produce and consume energy. A reduction in greenhouse gas emissions has become crucial especially with regards to the energy sector, which accounts for a staggering 75% of the emissions [2]. To achieve meaningful progress towards net-zero emissions, transitioning from fossil fuel-based energy onto more sustainable alternatives is the desire.

Among the emerging alternatives, nuclear energy stands out as one of the most promising solution. Nuclear power plants offer several key advantages, including the production of virtually zero emissions, long operational lifespans, high energy generation capacity, and the ability to provide a stable and continuous power supply, which sets them apart from intermittent renewable energy sources [3]. However, it is important to acknowledge that nuclear power is not without its challenges. Nuclear plants face significant hurdles in terms of cost, safety, siting, and regulatory licensing [4].

The construction and operation of nuclear power plants involve substantial upfront costs due to the use of high-quality materials and rigorous safety standards. Safety concerns related to nuclear accidents have driven the need for strong regulations and oversight [4]. Moreover, the selection of suitable locations for nuclear facilities often poses challenges due to proximity to population centers and environmental factors. Addressing these issues and ensuring the sustainability of nuclear energy in a changing energy landscape requires an innovative solution.

1.2 Small Modular Reactors

In the pursuit of cleaner and more sustainable energy sources, the concept of Small Modular Reactors (SMRs) has gained significant attention and recognition. SMRs are advanced nuclear reactors that produce electrical power typically at a scale of less than 300 Megawatt Electric (MWe) [5]. These compact reactors offer a range of advantages that make them

particularly appealing for a variety of applications, including the innovative OFNP, as we will explore in the following section.

The distinguishing features of SMRs include their reduced size compared to traditional nuclear power plants, less frequent refueling requirements, and inherent modularity. Their smaller power rating, approximately one-third the size of conventional reactors, contributes to cost savings and flexibility in deployment [5]. Furthermore, the modular nature of SMRs allows for their fabrication, transportation, and assembly in non-traditional locations, such as offshore nuclear platforms.

1.2.1 Types of SMRs

SMRs encompass a diverse array of reactor designs, each tailored to specific operational requirements and objectives. The various types of SMRs, include:

1. Light Water Reactor (LWR)s: LWR-based SMRs utilize light water as both a coolant and a neutron moderator. They are the most popular choice for many SMR projects as they have proven operational experience [6].

2. Gas Cooled Reactor (GCR)s: Gas-cooled SMRs employ gases such as helium or carbon dioxide as coolants. These reactors are the second most popular as they can operate at much higher temperatures than LWRs [6].

3. Liquid Metal Cooled Reactors: Liquid metal-cooled SMRs use liquid metals like sodium or lead-bismuth as coolants. These reactors offer advantages such as excellent heat transfer properties [7].

4. Molten Salt Reactors: Molten salt SMRs utilize liquid fluoride or chloride salts as both coolants and fuel carriers. These reactors can operate at high temperature and low pressure and offer a higher thermal efficiency [8].

Previous work in this field assumed that the OFNP would be modeled after LWR SMRs. However, this thesis marks a departure from that assumption exploring the use of Gas-Cooled SMRs. Now that we have introduced the concept of SMRs and highlighted the shift towards Gas-Cooled SMRs, we will delve into the specifics of the OFNP and its integration with the fuel transfer system.

1.3 The Offshore Nuclear Platform

Massachusetts Institute of Technology (MIT) has embarked on an initiative known as the Offshore Nuclear Plant OFNP. This concept integrates the design principles of SMR with the structural framework of an offshore oil platform [4]. The OFNP is a floating platform positioned in territorial waters adjacent to various coastlines, with the capability to transmit electrical power through underwater transmission lines. The offshore location of the OFNP offers distinct advantages. It mitigates many of the cost, safety, and licensing concerns commonly associated with land-based nuclear facilities.

Figure 1.1: Goliat [11]

The OFNP drew inspiration from SEVAN, a company known for designing cylindrically-shaped Floating Platform Storage Offloading (FPSO) vessels. Two notable platform types assessed as the principle hull designs for the OFNP design were SEVAN's platforms known as Voyageur Spirit and Goliat [9]. Figure 1.1 depicts the Goliat cylindrical hull shape as its being transported to sea. These platforms are known for exhibiting positive stability and versatility characteristics in varying sea states. The key difference between SEVAN and the OFNP developed is the OFNP has a more elongated hull and an additional section placed at the keel of the platform called the skirt to provide more stability for the platform [9]. The conceptual OFNP 300 and OFNP 1100 were designed to accommodate 300MWe and 1100MWe reactors, respectively. The initial layout with a LWR onboard OFNP 300 and 1100 are shown in Figure 1.2 respectively. Table 1.1 below details specifications for both OFNPs [10].

Table 1.1: Outline of OFNP platform characteristics [10]

Parameter	**OFNP300**	**OFNP1100**
Hull/skirt diameter (m)	45/75	75/106
Draft (m)	48.5	68
Total height (m)	73	108
Main deck height (m)	12.5	34
Displacement (tonnes)	~115,500	~376,400
Structural concrete (tonnes/MWe)	~5.8	~24.7

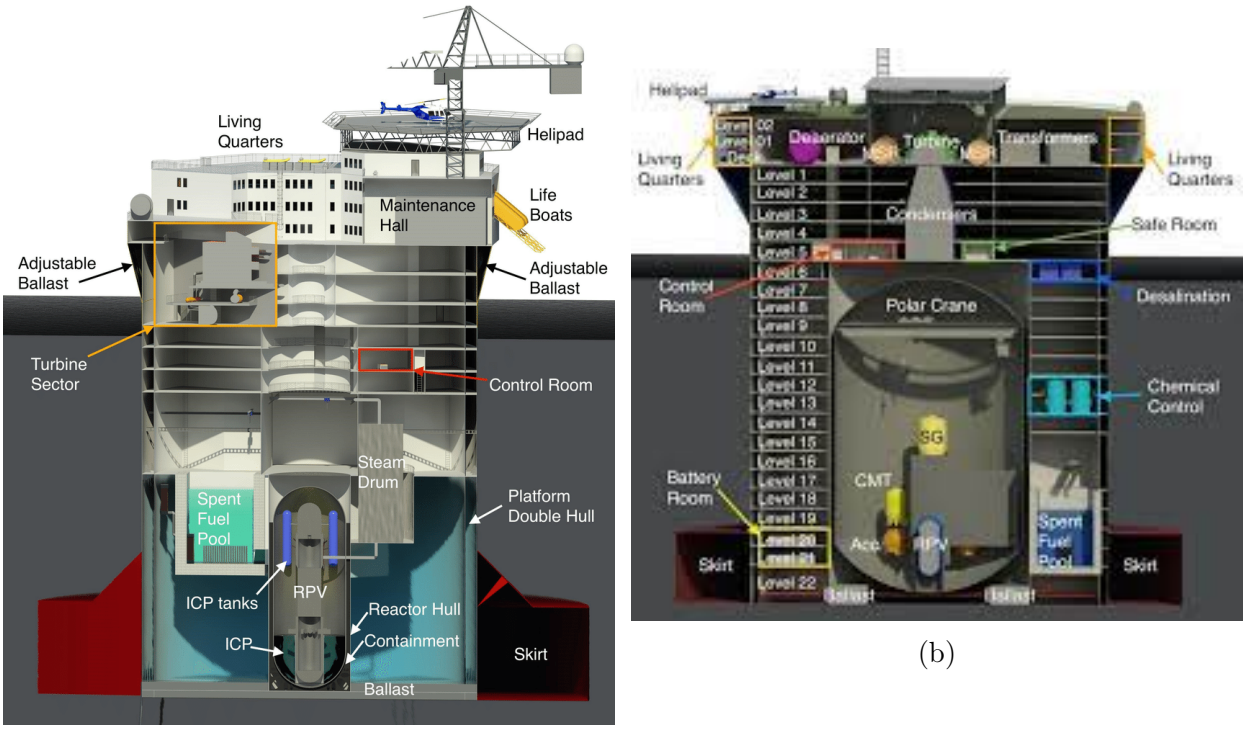

(a) (b)

Figure 1.2: A figure with two subfigures: (a) OFNP 300; (b) OFNP 1100. [9]

1.4 Problem Statement and Research Objectives

1.4.1 Problem Statement

The deployment of nuclear power generation in offshore environments, illustrated by the OFNP concept, presents a unique set of challenges. Among these challenges, the design and implementation of a specialized fueling infrastructure for the OFNP is key. The successful operation of the OFNP relies on a fueling system that can safely and efficiently support the continuous operation of its SMR in an offshore environment.

The commercial refueling processes employed in land-based nuclear plants may not be directly transferable to the OFNP's design and offshore setting, primarily due to the limited space available on the platform. This spatial limitation poses challenges in handling and maneuvering fuel rods, which are key components of nuclear refueling operations. Unlike land-based facilities, which often have the luxury of expansive areas for the movement and storage of fuel rods, an offshore platform must operate within much tighter constraints. The equipment typically used in land-based plants, including large cranes for removing and transporting fuel rods, may be impractically large for the confined spaces of a marine-based structure. Consequently, there development of a feasible and conceptually proven fueling infrastructure that meets the OFNP's specific requirements was necessitated.

1.4.2 Research Objectives

The primary objective of this thesis is to address the challenges associated with the design and implementation of a feasible and conceptually proven fueling infrastructure for the OFNP, considering key factors such as shielding, cooling, and size constraints. To accomplish this overarching goal, the following specific research objectives have been identified:

1. Conceptual Design: Develop a conceptual design for a fueling infrastructure tailored to the unique requirements of the OFNP, with particular attention to shielding, cooling systems, size and weight constraints. Prioritize feasibility and proof of concept while considering safety, efficiency, and compatibility with the OFNP's operational environment.

2. Proof of Concept: Explore and validate the feasibility of the proposed fueling infrastructure concept, emphasizing shielding effectiveness, cooling system functionality, and general arrangements. Demonstrate its practicality and safety in an offshore setting.

3. Safety Assessment: Conduct an initial safety assessment of the proposed fueling infrastructure, focusing on shielding mechanisms, cooling system safety, and monitoring equipment to maintain control throughout the fuel handling transfer process. Identify and address potential risks associated with fuel handling and transfer.

4. Feasibility Study: Perform a comprehensive feasibility study to evaluate the practicality and viability of the conceptual fueling infrastructure, taking into account factors such as, system arrangements, seakeeping and stability feasibility.

1.5 Scope of the Research

This research will focus exclusively on the development of a feasible and conceptually proven design for the fueling infrastructure of the OFNP. The primary aim is to establish the feasibility and viability of the fueling infrastructure concept within the context of the OFNP, while meeting the specified shielding, cooling, and size constraints. Practical implementation and optimization aspects, as well as full-scale operational considerations, fall outside the scope of this study.

1.6 Thesis Outline

The goal of this thesis is to design a feasible and conceptually proven refueling infrastructure onboard the OFNP. This infrastructure is specifically engineered to support continuous refueling operations, including the offloading of spent fuel, throughout the OFNP's anticipated 40-year operating period. The OFNP represents an innovative approach to nuclear energy production, integrating SMRs with offshore structures. In this context, the preferred SMR type for the refueling infrastructure is Gas-Cooled SMRs.

- Chapter 1 sets the stage by providing background information on the combating climate change by transitioning towards cleaner energy sources. It emphasizes the significance of nuclear energy, particularly SMR. Additionally, it introduces the concept of the OFNP, outlines the problem statement, and articulates the research objectives.
- Chapter 2 conducts a literature review focusing on fuel types of SMR, then focusing on both historical and present dayHigh Temperature Gas Reactor (HTGR). As fuel storage and transportation are the primary focus for this thesis the final portions of the literature review studies methods of spent fuel storage and ship to ship transfers.
- Chapter 3 highlights the design of the OFNP to include reactor and generator selections and the spent fuel storage architecture and supporting systems.
- Chapter 4 describes the fuel handling and transport systems. This includes the internal fuel handling, initial and final at sea transport design, and considerations for reactor decommissioning and defueling.
- In Chapter 5 describes a the feasibility analysis conducted covering structural, stability, seakeeping and shielding requirements throughout the transportation and handling system.
- Finally, Chapter 6 provides recommendations for future research and summarizes the key findings of the thesis regarding the feasibility of the refueling infrastructure for the OFNP.

Chapter 2

Literature Review

2.1 Fuel Types

In Chapter 1, a comparison is made between traditional light water reactors and high temperature gas reactors, focusing on the advantages and management of pebble bed reactors. This section dives into the various reactor fuel types, providing context to understand the design considerations for the fuel transport system.

2.1.1 Fuel Rods

Fuel rods are a common fuel form in traditional light water reactors. Fuel pellets, made of Uranium dioxide (UO_2) are stacked into a zirconium alloy pipe referred to as a fuel rod [12] [13] . The burnup of fuel rods ranges from 40 to 60 gigawatt days per ton of Uranium (GWd/tU) [3]. Bundles of these rods, known as fuel assemblies, spanning 4 meters in height making removal challenging [14].

2.1.2 Prismatic Fuel Assemblies

In contrast, some high temperature gas reactors utilize prismatic fuel elements, featuring compact configurations of TRISO fuel pebbles embedded in graphite blocks. These fuel elements typically have dimensions of approximately 360mm in diameter and 800mm in length [15]. The prismatic fuel compacts TRISO particles which are comprised of Uranium dioxide (UO_2) fuel kernels which are then coated with layers of carbon and ceramic materials.

2.1.3 Spherical Fuel Pebbles

Spherical TRISO fuel pebbles represent another fuel type used in high temperature gas reactors. Similar to prismatic blocks, TRISO fuel pebbles consist of uranium dioxide (UO_2) or Uranium OxyCarbide (UCO) kernels, coated with layers of carbon and ceramic materials. TRISO fuel pebbles are 60mm in diameter with a burnup rate of 90,000 MWd/tU [16]. Notably, TRISO fuel pebbles facilitate active refueling through recirculation while the reactor remains operational, an advantage over light water reactors that require shutdowns for refueling operations.

Each fuel type is shown in Figure 2.1 comparing the size and orientation between each of the fuel forms.

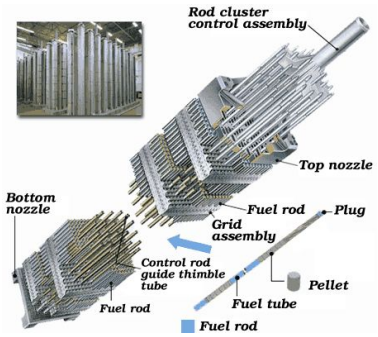

(a) Fuel Rod Assembly [3]

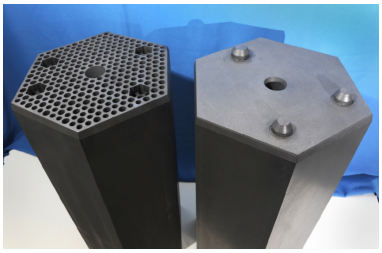

(b) Prismatic Fuel Assemblies [17]

(c) Spherical Fuel Pebbles [18]

Figure 2.1: Fuel types side by side for comparison

2.2 Historical High Temperature Gas Reactors

The historical development of HTGR underwent significant advancements through contributions from the United Kingdom, Germany, and the United States.

2.2.1 United Kingdom High Temperature Gas Reactors

The evolution of High Temperature Gas Reactors (HTGR) was traced back to the United Kingdom's Dragon Reactor, which was commissioned in 1964. Featuring graphite moderation and helium cooling, this pioneering reactor marked a significant milestone in HTGR development [19]. It utilized Tri-Structural Isotropic (TRISO) fuel within a prismatic hexagonal graphite structure consisting of 37 hexagons. The primary aim of the Dragon Reactor was to demonstrate the feasibility of high-temperature gas-cooled reactor technology for electricity generation [20]. Despite its innovative design, the reactor faced challenges related to fuel integrity and control rod performance during its operation and was eventually decommissioned in 1976 [21].

2.2.2 Germany High Temperature Gas Reactors

Germany further advanced HTGR technology with the introduction of the AVR reactor. Operating successfully for nearly 21 years, from 1967 to 1988, the AVR reactor represented a significant leap forward in HTGR design. The reactor's purpose was to prove the "functionality of a gas-cooled, graphite-moderated high-pressure reactor with spherical fuel elements" [22]. Despite the challenges encountered, the AVR reactor successfully demonstrated the feasibility of fuel pebbles [22]. Additionally, Germany's THTR-300 reactor undertook the task of evaluating a Pebble Bed Reactor (PBR) at a full-scale 300MWe, which was proven over a six-year operational span [23].

2.2.3 United States High Temperature Gas Reactors

In a similar vein to Germany, the United States operated a HTGR with a prismatic fuel assembles as the fuel type known as Fort St. Vrain [24]. This reactor was in operation from 1979 to 1989 before being decommissioned. It represented the United States' attempt to demonstrate the feasibility of a HTGR being used for electrical generation, operating out of Colorado as the first and only nuclear-operated reactor in the state [25].

Despite the challenges faced by these reactors, they collectively demonstrated the viability of HTGR. This led to the evolution of PBR technology, paving the way for the advancements seen in present-day reactor designs.

2.3 Current High Temperature Gas Reactors

The landscape of HTGR encompasses a variety of designs across different countries today. Notable examples include China's HTR-PM, and the United States' Xe-100, each with its distinct features and approaches to PBR technology.

2.3.1 China HTR-PM

China's HTR-PM is operational, having been connected to the grid in 2021. Following the legacy of its predecessors, its pebble bed design utilizes helium as a coolant, graphite as a moderator, and TRISO (UO_2) as the fuel composition. The HTR-PM consists of two ($250MW_{th}$) reactors coupled with a 210 MWe turbine generator. The reactor's design adopts an indirect steam cycle, achieving an electrical efficiency of 42% [26]. For spent fuel storage, a dry cask system is used.

2.3.2 United States Xe-100

In contrast, the United States' Xe-100 PBR, while not yet operational, is designed using UCO as its fuel source, achieving a burnup of 168,000 MWd/tHM. Rated at ($200MW_{th}$) and 80 MWe, the Xe-100's modular design can be expanded up to four reactors for a 320 MWe output. Unlike China's approach for the spent fuel storage cooling system, the Xe-100 spent fuel cooling system maintains a passive ventilation system rather than an active[16].

2.4 Spent Fuel Storage Methods

Spent fuel storage is a critical component of nuclear power plant operations, focusing on the safe containment and effective management of radioactive materials. There are two primary methods of spent fuel storage: wet storage and dry storage. Figure 2.2 illustrates these methods, with a spent fuel pool shown on the left demonstrating how fuel is kept submerged in water to cool and shield it, and a dry storage cask on the right showing how fuel can be securely enclosed in a sealed container that is both air-cooled and radiation-shielded.

2.4.1 Wet Storage

Wet storage involves the use of a spent fuel pool, 12 meters deep located within the nuclear power plant facility. This method is commonly utilized by traditional LWR as it provides several benefits, including efficient cooling and radiation shielding for workers. The requirements for wet storage include maintaining the pool at a specific temperature to prevent water from boiling off via circulation pumps and providing provisions for the eventual transfer of assemblies to dry storage, often facilitated by large cranes [27].

2.4.2 Dry Storage

In contrast, dry storage systems use canisters and casks to store spent fuel outside of the reactor containment building. This method is commonly employed by pebble bed reactors and other advanced reactor designs. In dry storage, spent fuel assemblies are placed within robust canisters and then further encapsulated within casks, silos, or wells for additional protection and storage flexibility [27]. Dry storage offers advantages such as reduced reliance on water cooling and the ability to store fuel assemblies in diverse locations, enhancing overall plant safety and security.

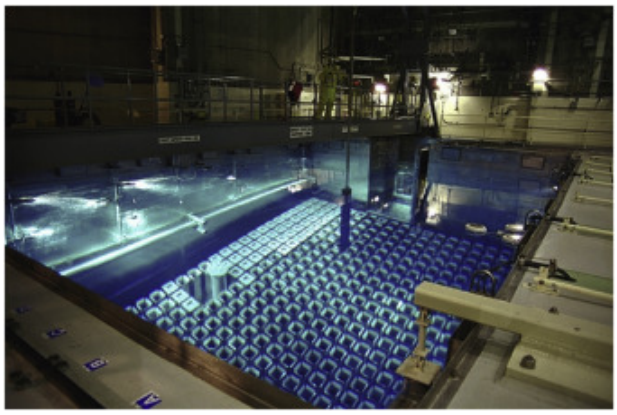

(a)

(b)

Figure 2.2: (a) Wet Storage [28]; (b) Dry Storage [29].

2.5 Ship to Ship Transfers

2.5.1 Introduction

STS transfer operations date back to the 1960s, typically involving the transfer of cargo, liquid, or gas between two seagoing ships due to the draft limitations of Very Large Crude Carrier (VLCC) and Ultra Large Crude Carrier (ULCC) with Deadweight Tonnage (DWT) spanning between 250,000 and 500,000 tons respectively [30] [31]. Two types of evolutions can occur during STS transfers: Lightering, where a VLCC transfers cargo onto a shuttle tanker, and Reverse Lightering, where the shuttle tanker transfers cargo onto the VLCC [30].

2.5.2 Anchored Ship to Ship Transfer Operations

Specialized STS operations are conducted while a VLCC or ULCC is at anchor. The stages of these evolution's are as follows:

1. Pre-Arrival Planning: In this stage, vessels verify compatibility, regulatory permission is received to conduct operations, and a joint operation plan is developed [32].

2. Approach and mooring: During this stage, environmental conditions are assessed, and the VLCC equips itself with pneumatic fenders in preparation for the mooring evolution. Tugs are positioned alongside the VLCC as well as the shuttle tanker to limit the relative motions of the VLCC and to safely position the shuttle tanker alongside the VLCC. Once positioned, vessels are moored, connecting cables from the VLCC to the shuttle tanker as seen in Figure 2.3a [33].

3. Cargo Transfer: Connections are made and the transfer of cargo is conducted [32].

4. Departure: Transfer equipment is disconnected, ships are unmoored, and with the aid of tugs, vessels are unberthed [33].

2.5.3 Case Study: STS Offloading Between Cylindrical Sevan Type-FPSO and Shuttle Tanker

A study was conducted to assess the conditions of STS offloading between an 87,900-DWT cylindrical Sevan type-FPSO and a 35,000 DWT shuttle tanker, which provided a dynamic analysis of STS transfers in anchored conditions. Figure 2.3a shows such STS operations between the Sevan platform and shuttle tanker. The Sevan platform, was equipped with a specialized mooring system consisting of 12 lines in three groups as shown in Figure 2.3b. The study assessed various wave headings 0°, 45°, 90°, 135°, and 180° considering the symmetric design of the Sevan platform. It concluded that STS operations can be safely conducted with wave heights up to 2.0 meters. This ensures that there are no excessive roll and pitch motions for either platform that would cause extreme tensions on the mooring lines, potentially leading to their breaking and the detachment of the fuel transfer system [34].

(a)

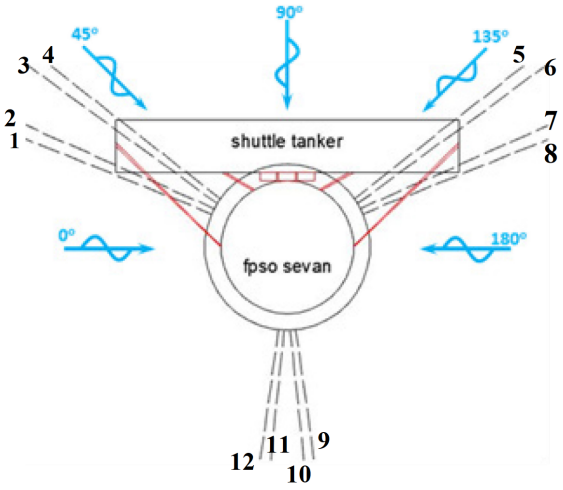

(b)

Figure 2.3: (a) Ship to Ship Transfer [35]; (b) Mooring Configuration [34].

Chapter 3

Design of Offshore Nuclear Platform

3.1 Introduction

In this chapter, we explore the decisions involved in selecting the OFNP 1100 platform and the PBR, specifically the HTR-PM model, for the OFNP. These choices are central in defining the fuel transport system, driven by the distinct advantages and operational efficiencies they provide.

3.1.1 Platform Selection

The OFNP 1100 platform is particularly suited to accommodate the PBR due to its capability for high-volume spent fuel storage, a critical requirement given the unique characteristics and fuel management needs of pebble bed reactors. However, this platform is not the most economical choice, as it is being utilized for a 210MWe reactor rather than the 1100MWe capacity it was originally designed for. Nevertheless, the large spent fuel storage capacity, structural integrity and stability of the OFNP 1100 affirm its ability for this application. Some specifications of the OFNP 1100 can be found in Chapter 1, Table 1.1.

3.2 Reactor and Generator Selection

3.2.1 Reactor Selection Process

Drawing on the literature review presented in Chapter 2, the selection process for the reactor type is guided by an evaluation of fuel types and reactor refueling management. The decision to adopt a PBR, specifically modeled after China's HTR-PM reactor, is influenced by several factors:

- **Compact Fuel Form and At-Power Fuel Replenishment:** The PBR is notable for its use of spherical fuel pebbles and the capability for continuous fuel replenishment during operation. These features enable the handling and transportation of spent fuel without disrupting the electrical power supply to the grid. For an illustrative example, a front view of the HTR-10 reactor, the test PBR that inspired the HTR-PM design,

is shown in Figure 3.1 [36]. Detailed descriptions of the reactor and fuel characteristics are provided in Tables 3.1 and 3.2.

- **Safety Mechanisms and Operational Advantages:** The design features of the HTR-PM, including its use of helium as a coolant and graphite as a moderator, combined with inherent safety mechanisms such as negative temperature coefficients and limited chemical reactions due to inertness of helium, reinforce its selection.

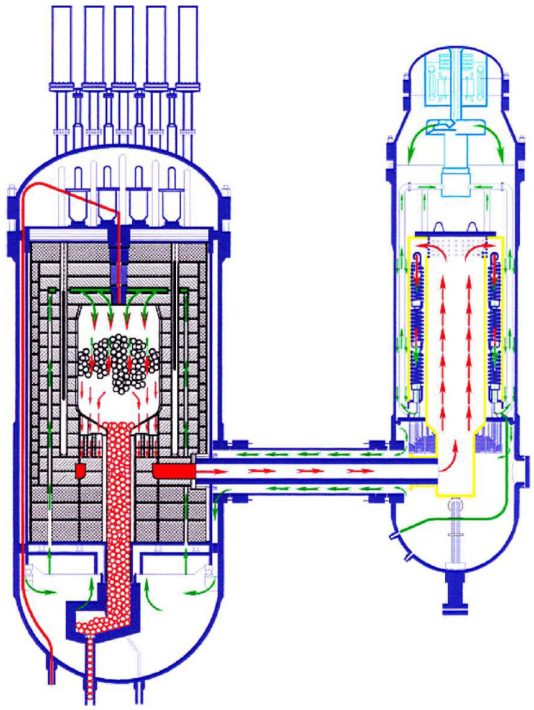

Figure 3.1: Front View of HTR-10 Reactor [36]

Table 3.1: Reactor Characteristics [36] [26]

Parameter	**Value**
Electrical Power (MWe)	210
Thermal Power (MWth)	2x250
Designed Lifetime (years)	40
Electrical Efficiency (%)	42
Thermodynamic Efficiency (%)	40
Reactor Core Dimensions (m)	Diameter: 3, Height: 11
Weight (tonnes)	700
Fuel Spheres in Core	420,000
Fuel Circulated Per Day	6,000

Table 3.2: Fuel Characteristics [26][37]

Parameter	Value
Fuel type TRISO	(UO2)
Fuel Element Loading (max) (gU/FE)	7
Enrichment of fresh fuel (%)	8.5
Fuel Sphere Diameter (m)	0.06
Fuel Sphere Volume (m^3)	0.000113
Fuel Burnup (MWd/tHM)	90000
Max Fuel Sphere Power (kW)	1.8
Average Fuel Sphere Power (kW)	0.60
Total Density (kg/cm^3)	1769.91
Total Mass (kg)	0.2

3.2.2 Generator Selection

The power generation system of the OFNP employs a M501G Series turbine generator [38]. This turbine generator is capable of providing the required 250MW of power and is designed to fit within the platform's specifications. The characteristics of this turbine generator are detailed in the table provided.

Table 3.3: Generator Characteristics [38]

Parameter	Value
Type	Mitsubishi M501G Series
Length (m)	12.9
Width (m)	5.1
Height (m)	5.5
Rated Power (MW)	427
Weight (tonnes)	295

3.3 Spent Fuel Storage Design

The onboard storage segment of the platform design centers on three key aspects: the methodology of spent fuel storage, the storage capacity of the spent fuel room, and the cooling and shielding considerations.

To facilitate the efficient removal of spent fuel, the design integrates dual-purpose transport casks. These casks are specifically selected for their capability to store and transport fuel off the hull. The Holtec HI-STAR 100 cask, chosen for its vertical orientation and dual-purpose features, serves as an example [39]. As described in Chapter 2, casks are used in conjunction with fuel canisters that hold the fuel. The dimensions of this cask dictate the necessary canister size to ensure compatibility with the cask's internal diameter. The HTR-PM canister satisfies these conditions, as demonstrated in Table 3.4, and is the canister used

for this design. Figure 3.2 provides a visual representation of the HTR-PM canister and Holtec HI-STAR 100 Cask.

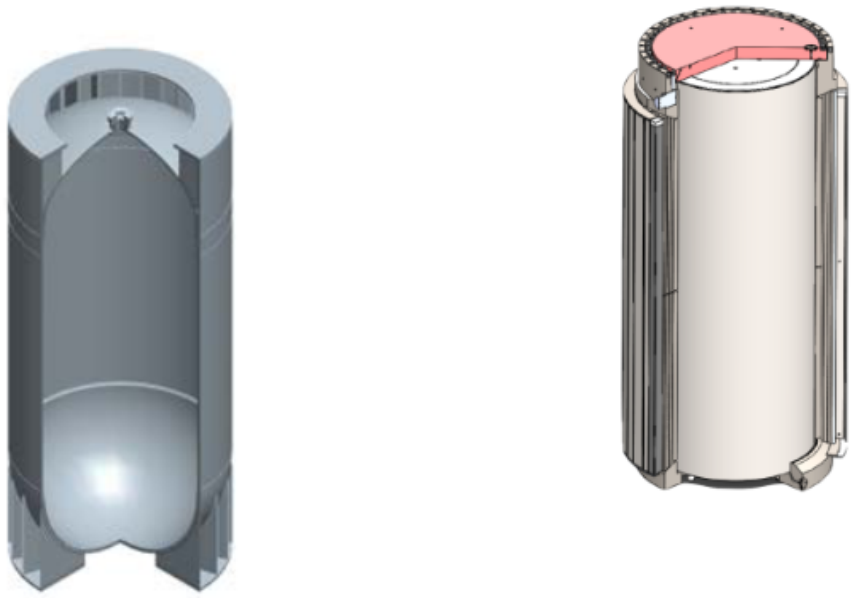

(a) Canister [40] (b) Transport Cask [41]

Figure 3.2: (a) Spent Fuel Canister; (b) Spent Fuel Cask.

Table 3.4: Combined Characteristics of Canisters and HI-STAR 100 Casks [39], [42]

Parameter	**Canister Value**	**Cask Value**
Diameter (m)	1.78	2.43
Height (m)	4.18	5.15
Volume (m^3)	10.40	23.88
Weight Full (tonnes)	14	136.61
Weight Empty (tonnes)	6	76.5
Capacity (Pebbles)	40,000	40,000
Max Decay Power (kW)	27.1	-
Max Decay Density (kW/m^3)	3.65	-
Material	304_{SL}	304_{SL}
Spacing (m)	3	3
Post Irradiation Cooling Time (yrs)	5	5
Total Accumulated Pebbles (2 reactors)	1.46×10^7	1.46×10^7
Number of Canisters and Casks Required	37	37

The storage capacity of the spent fuel rooms aboard the OFNP is constrained by the generation of decay heat, which is the heat released as a result of radioactive decay [43]. Proper

management of decay heat is essential during storage periods and within cooling systems to prevent unsafe conditions on the platform. Compared to Pressurized Water Reactor (PWR) spent fuel rods are stored for a combined 15 year period before being transported to their final destination at a repository. However, the HTR-PM reactor design used in this concept discharges approximately 800 fuel pebbles per day, necessitating significant storage capacity to accommodate the required number of canisters and casks over a 15-year period. According to the study by Wang et al., a five-year storage capacity is feasible, assuming the decay heat level stabilizes at a relatively low 1.34 kW as shown in Table 3.5 and Figure 3.3 both show the exponential decay of the spent fuel pebbles over time [42]. With this assumption, storing spent fuel for five years would require approximately 37 canisters and casks. To simplify the design, provisions are made for 40 canisters and casks, which are distributed between two centrally located spent fuel rooms on the platform, with each room housing 20 pairs of canisters and casks.

Table 3.5: Decay Heat [42]

Time (years)	**Decay kW/canister**	**Avg. kW/Pebble**
5	1.34	3.35×10^{-5}
10	0.84	2.10×10^{-5}
50	0.32	8.00×10^{-6}

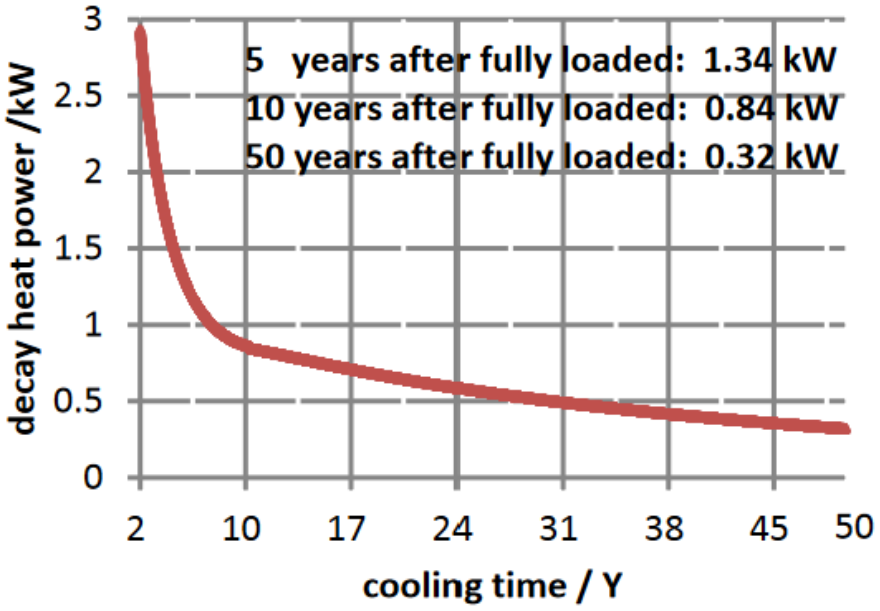

Figure 3.3: Decay Heat for Single Canister as assessed by HTR-PM Study, Wang et, al [40]

3.3.1 Cooling System

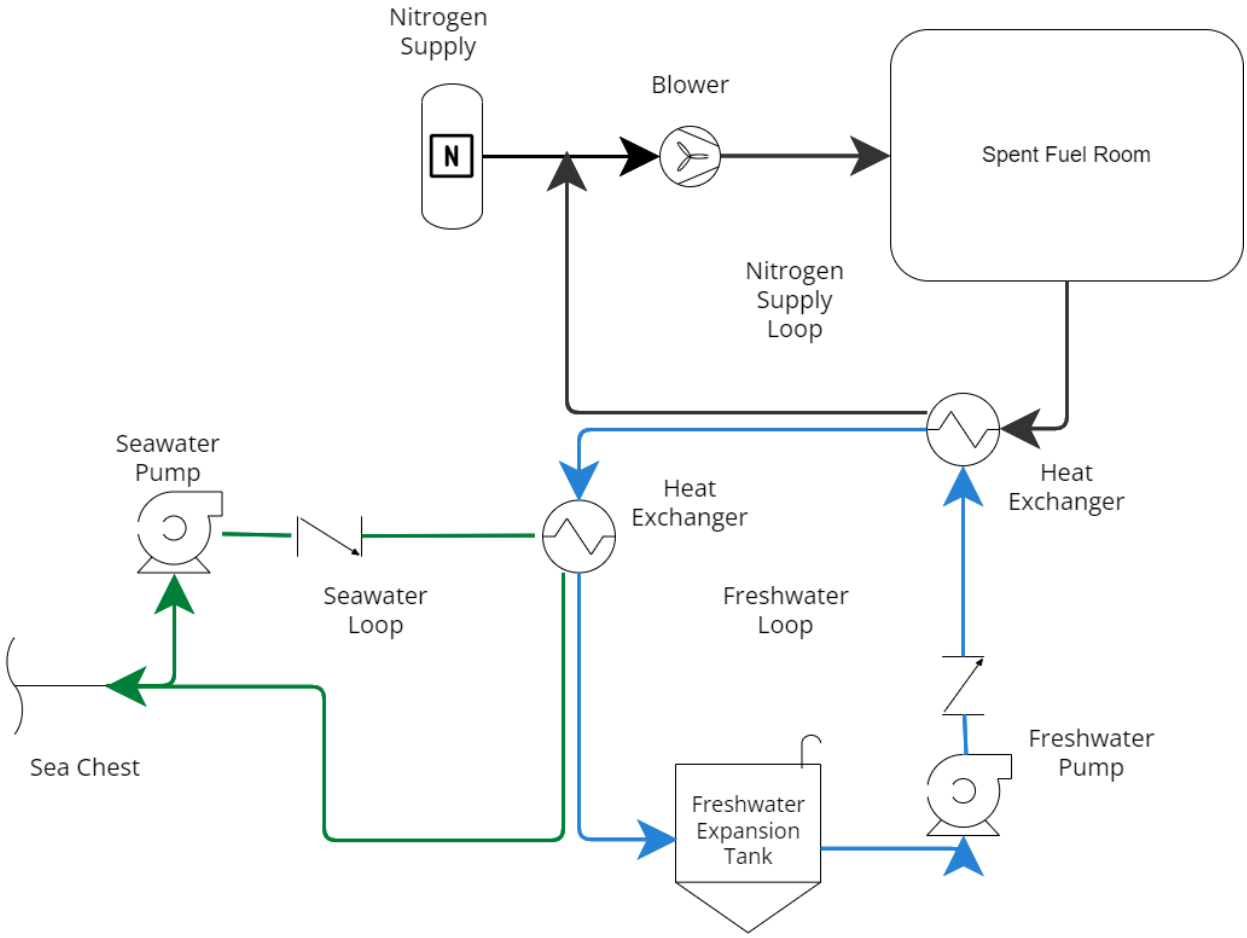

Figure 3.4: Schematic of Cooling System

Overview and System Layout Considerations A closed-loop cooling system is employed to manage the heat generated by 20 spent fuel canisters within each spent fuel room, where each canister generates 27.1 kW of decay heat, resulting in a total heat load of 542 kW. The system utilizes nitrogen, freshwater, and seawater to ensure efficient heat dissipation. Figure 3.4 provides the schematic of the cooling system, illustrating the placement of the Lamson 2400, as well as other common equipment such as heat exchangers and cooling pumps. To mitigate contamination risks and simplify maintenance, the system is strategically located in a separate room from the spent fuel canisters.

Heat Load Calculation The calculation for the total heat load required to be removed from the spent fuel room is as follows:

$$Q_{\text{load}} = n \times q_{\text{canister}} = 20 \times 27.1\,\text{kW} = 542\,\text{kW} \tag{3.1}$$

where n is the number of canisters and q_{canister} is the heat load of an individual canister.

System Components and Flow Rates The cooling system comprises blowers for circulating nitrogen and a two-stage heat exchanger system that facilitates the transfer of heat from the nitrogen to freshwater and then from freshwater to seawater, ensuring no cross-contamination into the ocean.

Blower Selection and Flow Rate A Lamson 2400 blower, with an inlet flow range of 22,100 to 70,100 m3/h, is selected to accommodate the system's requirements [44]. The necessary nitrogen flow rate to ensure adequate cooling is determined to be [45]:

$$\text{Nitrogen flow rate} = \frac{Q_{\text{load}}}{c_{\text{nitrogen}} \times \Delta T} \tag{3.2}$$

Given that c_{nitrogen} is the specific heat capacity of nitrogen, with a value of $1.04\,\text{J/kg}\cdot\text{K}$, and assuming a temperature change $\Delta T = 25\,^{\circ}\text{C}$, the necessary nitrogen flow calculation is as follows:

$$\text{Nitrogen flow rate} \approx 66,200\,\text{m}^3/\text{hr}$$

3.3.2 Shielding and Monitoring

The AP1000 CA20 Module's advanced modular design, measuring 20 meters in length, 14 meters in width, and 20 meters in height, serves as the prototype for the example spent fuel room within the OFNP [46]. The storage facility has been scaled to dimensions of 40 meters in length by 28 meters in width, maintaining the original height, to meet the OFNP specific storage demands for PBR fuel.

With this design expansion, the facility can now accommodate 20 canisters and 20 casks, arranged to ensure a clearance of 3 meters width wise and 2 meters lengthwise, allowing for autonomous equipment to be used in the room for maintenance or other accessing needs.

Originally, the CA20 Module, with a mass of 840 tonnes, utilized a shielding strategy comprising 1376 cubic meters of concrete [46]. This substantial concrete volume plays a role in ensuring radiation safety through effective attenuation of gamma and neutron radiation emanating from spent nuclear fuel. As we extrapolate this design to a larger volume, it's estimated that approximately 5600 cubic meters of concrete will be required for the new spent fuel room. Proportionally, this implies an anticipated total mass of 3418 tonnes for the shielding structure. For this design two of these rooms would be used onboard the OFNP to house the total 40 canisters and casks.

To enhance safety and monitoring capabilities, the design of the spent fuel room aboard the OFNP incorporates cameras, pressure, and temperature sensors. These additions enable remote monitoring from the control room, facilitating early detection of any issues, particularly in the ventilation system, to ensure safe temperature levels are maintained. Additionally, the room's layout includes a ground crane, such as the 150-tonne capacity cask handling cranes manufactured by Konecranes, which lifts canisters and casks as needed. This setup to include an image of the ground crane is detailed in Figures 3.5 [47].

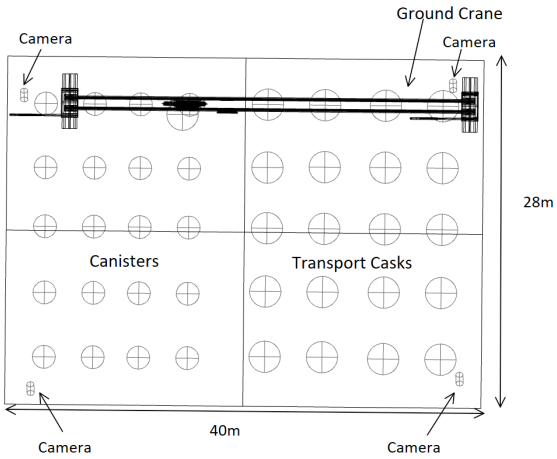

(a) Top View of Spent Fuel Room

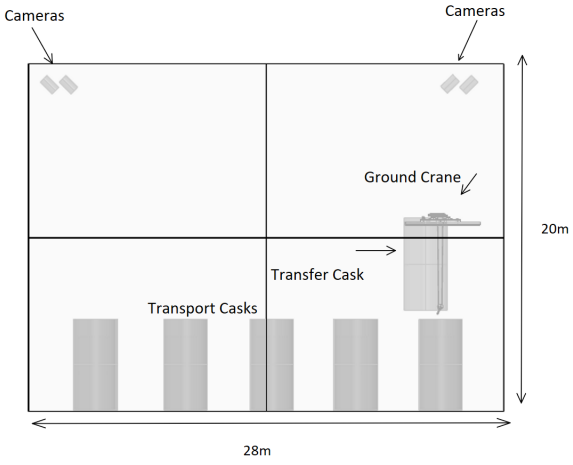

(b) Side View of Spent Fuel Room

(c) Ground Crane

Figure 3.5: (a) Top View of Spent Fuel Room with 20 canisters and casks; (b) Side View of Spent Fuel Room; (c) Ground Crane [47]

Chapter 4

Fuel Handling and Transport Design

4.1 Fuel Handling System

4.1.1 Introduction

For simplicity, the fuel handling system employed onboard the OFNP follows the design of the HTR-PM, which itself was inspired by the earlier HTR-10 model. Figure 4.1 provides a schematic representation of the fuel handling process as used in this context, and the details of this system are further explained below [48].

4.1.2 System Process Overview

The Fuel Handling System (FHS) is designed to manage the fuel cycle within the reactor autonomously. The process is as follows:

- **Initial Loading**: New fuel elements transit through the reactor core as part of the initial loading, facilitated by the fresh fuel room which refuels the reactor as needed through the supply of fresh fuel pebbles that are fed into the elevator and directed into the core as needed.
- **Circulation**: Fuel elements descend by gravity through the reactor core, undergoing fission and eventually collecting in a discharge tube.
- **Discharge and Sorting**:A helium gas stream, known as pulse gas, is used to individually guide fuel elements to a failed fuel separator. Here, the fuel elements are inspected, and any damaged elements are stored in a separate failed fuel canister.
- **Burn-up Measurement**: Intact fuel elements reach an elevator for burn-up measurement. Post-assessment, they are either recirculated to the core or diverted to a spent fuel buffer line through elevating helium gas, based on whether they have reached their burn-up limit.
- **Re-circulation or Disposal**:

- Partially depleted fuel elements are returned to the core via the elevating helium gas and blower for further energy generation.
- Spent fuel elements are sent to the spent fuel room, where they are loaded into spent fuel canisters. The rate at which the elements are discharged from the two 250MW reactors in this design is 800 elements per day.

- **Fresh Fuel Supplement**: Concurrent with the discharge of spent fuel, fresh fuel elements are introduced into the cycle to maintain a consistent fuel supply.

This FHS is the first step in preparing the fuel elements for at sea transport upon the 5 year decay storage period.

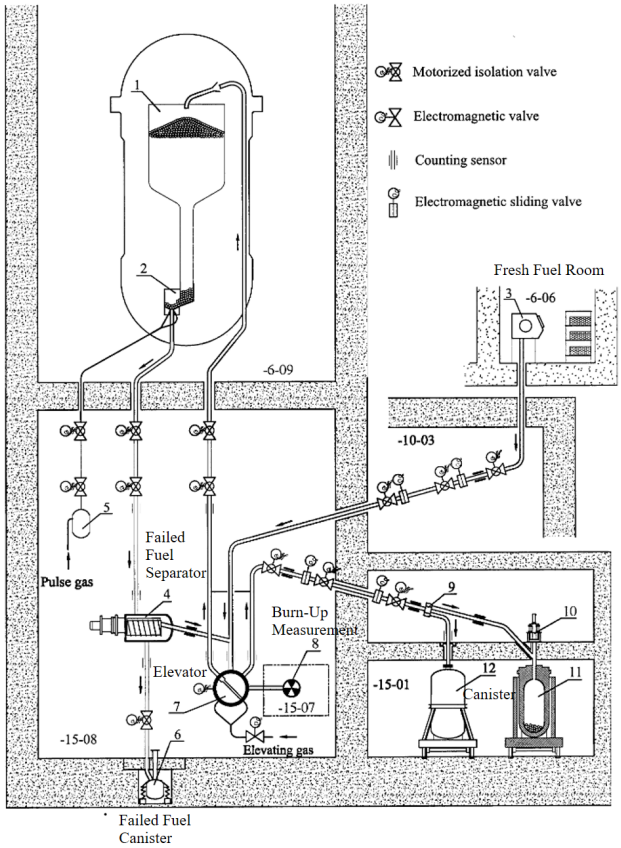

Figure 4.1: Schematic of the fuel handling system adapted for the OFNP.[48]

4.2 Design No. 1

4.2.1 Introduction

In Chapter 3, we explore the design of the spent fuel storage facility, which is designed to accommodate five years' worth of spent nuclear fuel. We assess two fuel transport designs; Figure 4.2 showcases design number one. Subsequent sections elaborate on the characteristics

of this design. Through our examination, several challenges emerge, leading to a decision to pause further development of the project.

Particularly, the total weight of the canister cask assembly, which is 90 tonnes, is elevated to a height of 108 meters. This elevation causes a shift in the platform's center of gravity. To counteract this shift and address the potential for excessive heel motion on the platform, a ballasting solution is necessary. The weight, when lifted on one side of the platform, places tension on the mooring line anchored to the seabed, which is used to maintain the platform's position. These significant changes prompt a reevaluation of the feasibility of continuing with this design without extensive research into platform stability operations.

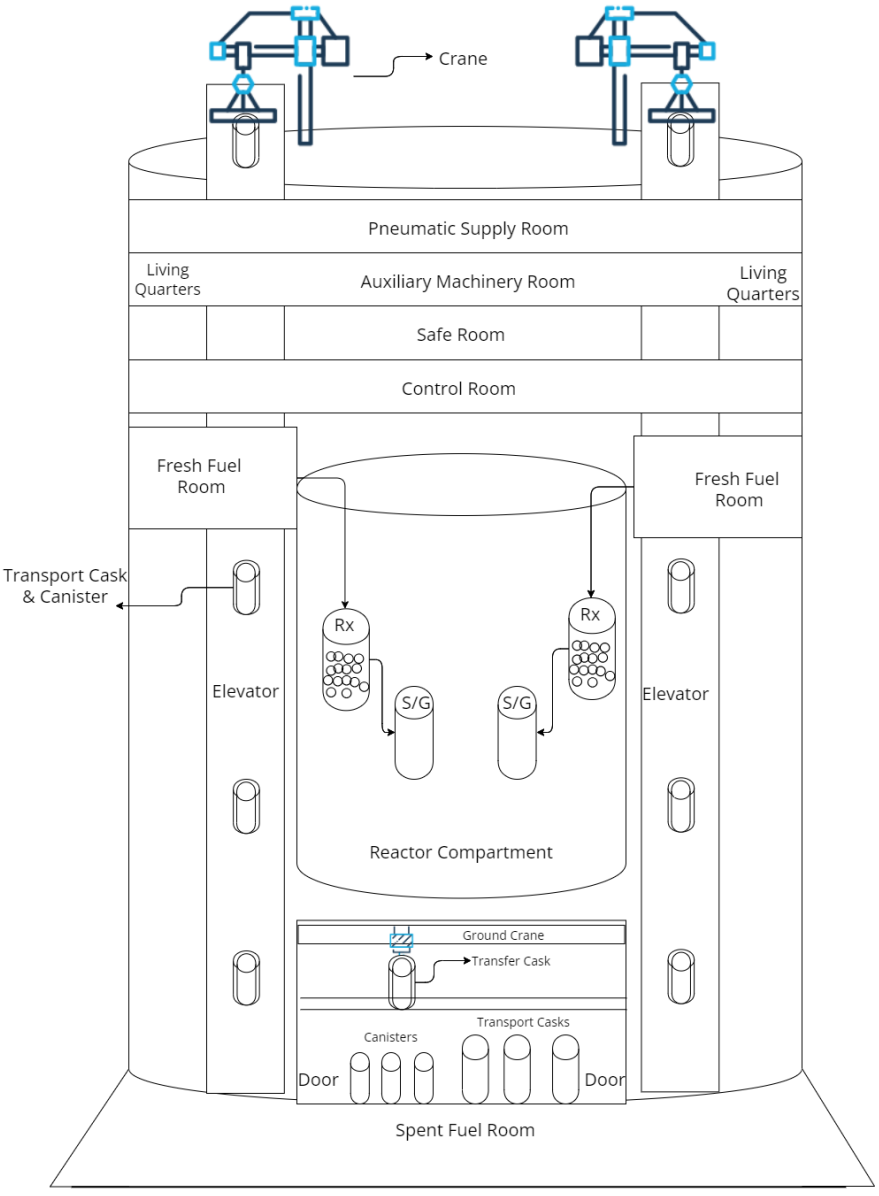

Figure 4.2: Cask Transport Flow Diagram

The design operates in three stages: retrieval, vertical transport, and horizontal trans-

port. These stages are as follows:

4.2.2 Retrieval

The retrieval of spent fuel casks marks the first stage in design number one.

- **Spent Fuel Room Process:** After the five-year storage period concludes, the oldest canister containing 40,000 pebbles is loaded into a transfer cask using a ground crane. This transfer cask acts as an overpack, providing additional shielding and maintaining positive control during the transfer into the dual-purpose transport cask. Figure 4.3 shows the canister transfer process, showing both the canister movement and placement of it within the transport cask. Of note, this design does not include interim storage of the spent fuel. Once the transfer cask with the canister inside is securely placed within the transport cask, the transfer cask is carefully removed, leaving the canister seated within the transport cask.

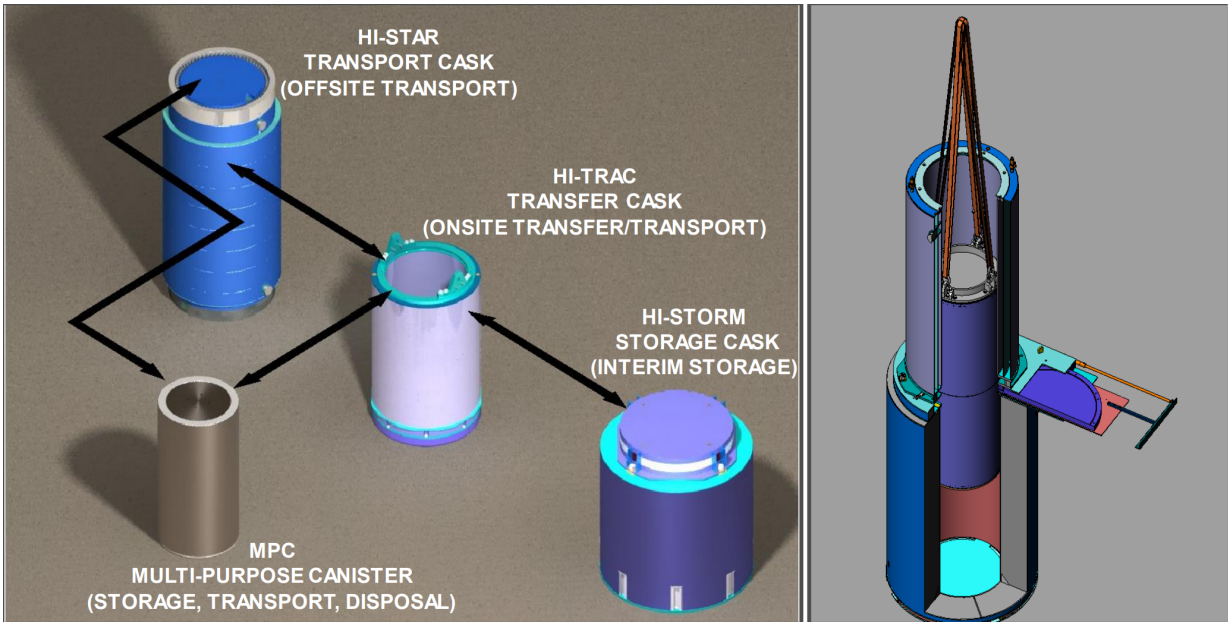

Figure 4.3: Canister Transfer Process [49]

- **Canister Sealing Process:** The canister is then welded shut using an automated gas-tungsten arc welding process, ensuring a airtight seal. This is needed for containing the radioactive materials and preventing any potential leaks [50].

- **Transport Cask Sealing Process:** After the canister is sealed, the transport cask is then sealed by a pneumatic system powered by compressed air is used to operate a claw mechanism. This claw is designed to handle and position a plug that seals the cask. Air pressure makes the claw open and close. It grips the plug and places it securely into the top of the cask, effectively sealing it to prevent any leakage of materials and to protect against external contaminants. Additional air-powered actions help tighten

the seal, ensuring the cask is completely airtight for safe storage and transport of the spent fuel. [48].

- **Transportation Preparation:** Once the transport cask containing the sealed canister is securely sealed, it is ready for relocation. The cask transporter, shown in Figure 4.4a, operated by trained personnel, is used to lift and move the cask out of the spent fuel room. Operators use a combination of manual controls and automated systems to ensure the cask is securely rigged to the transporter. This process involves precise maneuvering and careful attachment of the cask to the transporter's lifting mechanism, often with the aid of guidance systems and safety checks to prevent any mishandling. Due to the transporter's substantial dimensions—6 meters in height and 5 meters in width—the capacity of the spent fuel room has been adjusted from the initially proposed 40 canisters to 37. This reduction in capacity ensures there is sufficient clearance for the safe navigation of the transporter, facilitating the efficient and safe handling and transitioning of the casks to the elevator. This careful orchestration not only optimizes space within the spent fuel room but also enhances operational safety, as detailed in the operational guidelines [51].

4.2.3 Vertical Transport

Upon retrieval, the casks undergo vertical transportation, requiring a system with significant lifting capabilities and appropriate safety measures.

- **Vertical Lift Elevator:** An elevator for example engineered with a lift capacity of 100 tons comfortably handles the 90-ton weight of the dual purpose cask. To accommodate the cask transporter, the elevator is designed with a door width that allows the entry and placement of the cask. Once inside, the cask is securely positioned for vertical movement and the cask transporter retreats. A safety precaution of the elevator system for example is an automatic limit switch and an emergency brake system to prevent any unintended movements.

4.2.4 Horizontal Transport

Following the vertical ascent, casks are horizontally transferred to the main deck area of the platform. Here, another cask transporter repositions the cask from the elevator, before it is rigged to a crane for further handling. For example, a 150-ton MacGregor crane could be used for the task [52]. This crane then lifts the cask off the platform and onto a shuttle tanker. Given the substantial weight of the casks, a stability analysis is essential to ensure safe operations during heavy lifts over the side of the platform.

(a) Cask Transporter used to retrieve and place transport casks into the elevator.

(b) Macgregor 150 ton crane used for offloading the transport casks.

Figure 4.4: Illustrations of the transport equipment used in Design No.1 fuel transport process: (a) Cask Transporter; (b) Macgregor 150 ton crane. [51], [52]

4.2.5 Shielding

In design number one , significant attention is given to the evaluation of shielding measures. The design of the spent fuel storage and transportation process incorporates the use of transport casks that are engineered to ensure safe handling and minimize radiation exposure. These casks, once sealed, effectively contain the radiation, allowing for their safe maneuvering without posing any risk to personnel.

As a result, modifications to enhance the operation of the cask transporter, elevator, and crane are not necessary from a radiation safety perspective. From a monitoring perspective, the elevator will be equipped with cameras for ongoing monitoring to ensure secure vertical transport of spent fuel casks. The transport casks themselves are designed to provide adequate shielding, ensuring that once the spent fuel is sealed within these casks, they can be handled safely. This design approach effectively limits personnel exposure to radiation, and minimizing the need for additional protective measures during the handling and transport processes.

4.3 Design No.2

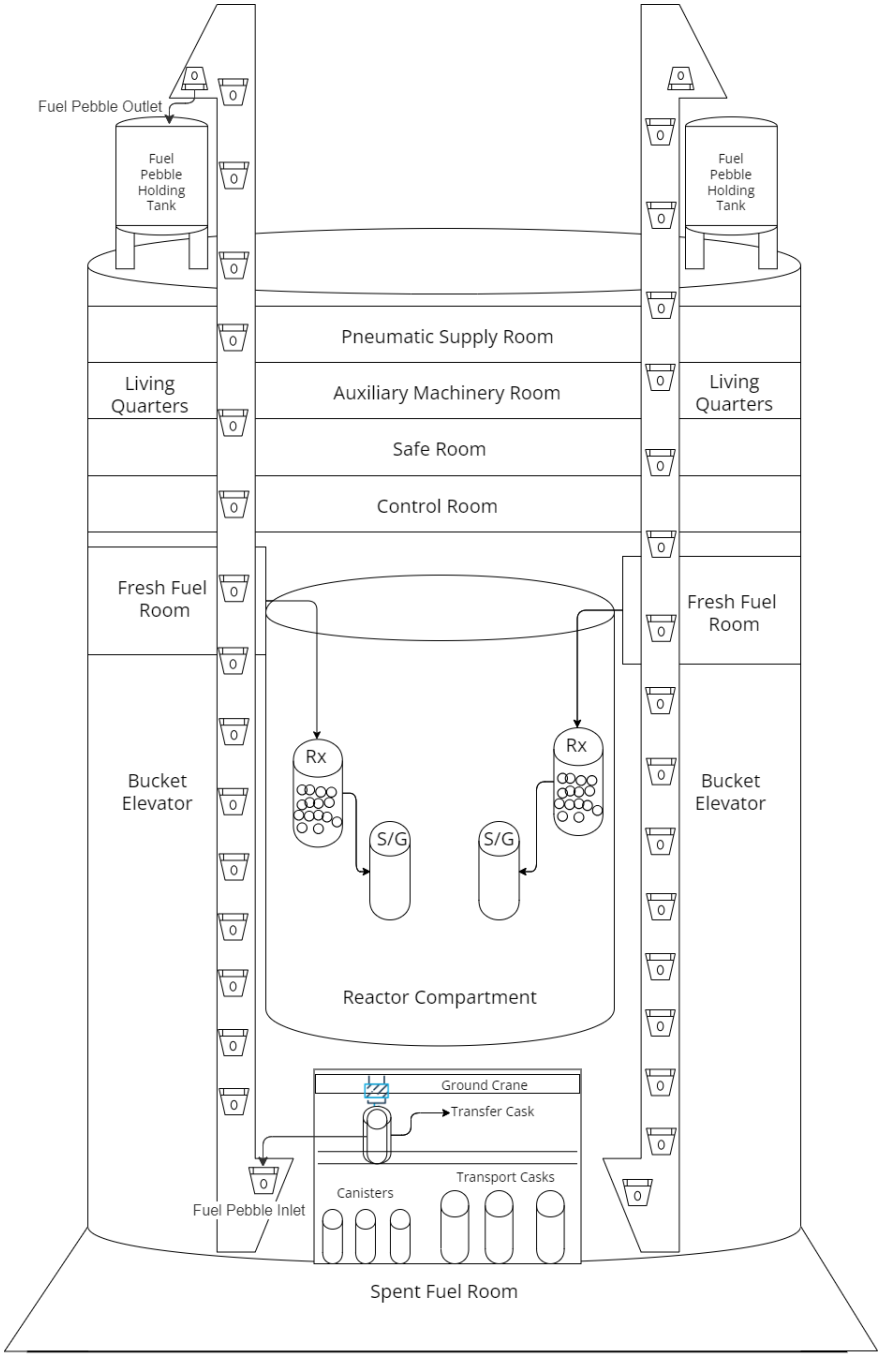

Figure 4.5: Fuel Pebble Flow Diagram

4.3.1 Introduction

Design number two involves transporting the fuel pebbles individually. Figure 4.5 illustrates the expected flow path for the fuel pebbles during at sea transport. This process begins with

a bucket elevator for vertical conveyance. Upon completion of the vertical transport, the pebbles are pneumatically conveyed off of the OFNP and onto a shuttle tanker. This tanker is specifically designed to receive the fuel pebbles and store them in dual-purpose casks, which are later offloaded onto an approved land facility for storage. Like design number one design, the design number two is also structured in three main stages: retrieval, vertical transport, and horizontal transport.

4.3.2 Retrieval

The retrieval stage is specifically designed to manage the safe and efficient collection of individual fuel pebbles for at-sea transportation.

- **Ground Crane:** The process begins with the use of a ground crane within the spent fuel room, which is utilized for maneuvering canisters and transfer casks around the room. Once a canister reaches its five-year decay period—making it suitable for at-sea transport—the ground crane places a transfer cask around the canister. Subsequently, the canister and transfer cask are both lifted to the filling shelf, where the canisters are initially filled with spent fuel during reactor operations.
- **Fuel Pebble Retrieval:** With the canister securely positioned within the transfer cask at the filling station, a retrieval device consisting of a pipe equipped with a rotary airlock to control the flow of the pebbles is inserted through a hole at the top of the canister's lid. An industrial centrifugal blower then applies vacuum suction to extract the fuel pebbles [42].
- **Helium-Assisted Transportation:** The extracted pebbles are conveyed through a pipeline that is integrated back into the fuel handling system. In this concept design, helium gas will propel the fuel pebbles throughout the FHS as needed. A pebble discharge pipeline added to the FHS will discharge the pebbles directly into the bucket elevators, ensuring that the pebbles are deposited into the bucket elevator at a controlled rate.

4.3.3 Vertical Transport

Upon the discharge of fuel pebbles into the bucket elevators, the buckets will ascend via a chain system to the main deck of the platform. The elevator as an example for the concept design, 108 meters in height and equipped with 900 buckets, holds 30 pebbles, totaling 27,000 pebbles per full trip. To transfer all 40,000 pebbles, approximately two full trips are required. At a speed of 0.25 m/s, it takes about 7.2 minutes to complete one ascent or descent, totaling about 15 minutes for a full round trip. Therefore, it will take approximately 30 minutes to transfer all 40,000 pebbles to the top of the platform and into a holding tank where they will be temporarily stored until it is time to horizontally transport the fuel pebbles off hull.

The selection of bucket elevators over traditional elevators is based on their proficiency in vertically conveying bulk materials with minimal loss and maximum efficiency, a common requirement across various industries such as agriculture and mining [53]. Gough Cahn, the manufacturer, designs heavy-duty bucket elevators that are ideal for this purpose. These

elevators are configured with specially oriented outlets, shown in Figure 4.6 to ensure precise and controlled discharge into a holding tank, crucial for maintaining control over the pebbles throughout the transport process.

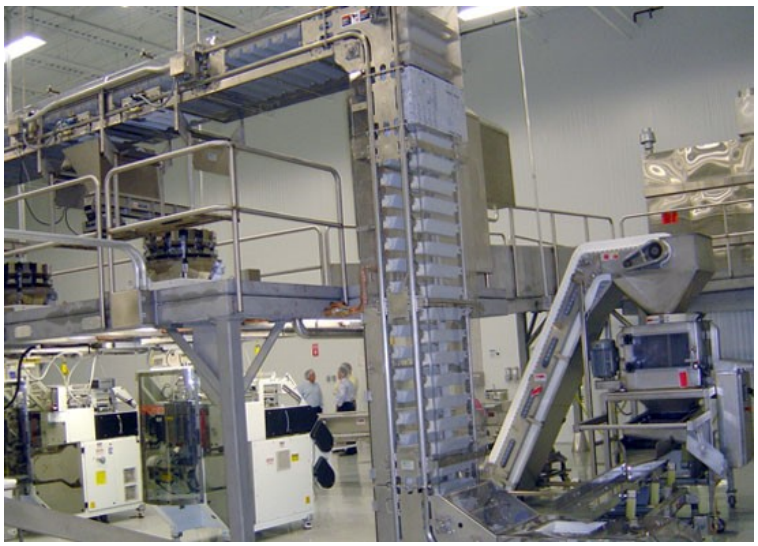

Figure 4.6: Heavy Duty Elevator Perspective View. [54]

Table 4.1: Specifications of Bucket Elevator [53][55]

Parameter	**Value**
Bucket Type	M-Series Bucket
Bucket Material	303SL
Temperature Limit ($°C$) [56]	425
Bucket Width (m)	0.22
Bucket Length (m)	0.23
Bucket Depth (m)	0.12
Conveyor Speed (m/s)	0.25
Bucket Capacity ($(m^3)/h$)	10.37
Working Loads (tonnes)	2.18
Tensile Strength (tonnes)	10.88
Fuel Pebble Volume (m^3)	1.13×10^{-4}
Bucket Volume (m^3)	6.07×10^{-3}
Number of Pebbles per Bucket (60% Fill)	32.21
Estimate Number of Buckets Needed	900

4.3.4 Horizontal Transport

The horizontal transport of fuel pebbles is the last phase in the the at-sea transport system and endures the highest risk as fuel pebbles are pneumatically propelled at sea. This stage utilizes a hose, enclosed within a gangway reinforced with carbon steel for shielding, to ensure

safe and efficient transfer operations during ship-to-ship (STS) interactions as discussed in Chapter 2.

Platform Configuration and System Connections The fuel pebbles are stored in a holding tank at the top of the OFNP until they are ready for horizontal transport. Before this can occur, the OFNP must be configured for STS operations. As discussed in Chapter 2, the OFNP and shuttle tanker are moored together using pneumatic fenders to maintain a safe mooring distance, as specified in Table 4.2. These fenders, selected based on a berthing coefficient that ensures compatibility with the tanker's operational load (outlined in Table 4.3, and Equation 4.1 [57]), support a coefficient of approximately 261,000 tonnes, aligning with load capacities between 200,000 and 330,000 tonnes, as illustrated in Figure 4.7.

Table 4.2: Pneumatic Fender Specifications [58]

Parameter	**Value**
Classification	Yokohama
Fender Diameter (m)	3.3
Fender Length (m)	10.6
Initial Internal Pressure (kPa)	80
Energy Absorption (kJ)	4281
Reaction Force (kN)	6907
Hull Pressure (kPa)	208
Number of Fenders Required	4

$$C_{\text{berthing coefficent}} = \frac{2 \times \text{DisplacementShipA} \times \text{DisplacementShipB}}{\text{DisplacementShipA} + \text{DisplacementShipB}}, \tag{4.1}$$

C Berthing Coefficient	Relative Velocity	Berthing Energy	Suggested Fenders	Typical Pneumatic Fender
Tonnes	M/Sec	Tonnes.m	Quantity	Meter
1,000	0.30	2.4	3 or more	1.0 x 2.0
3,000	0.30	7.0	〃	1.5 x 3.0
6,000	0.30	14.0	〃	2.5 x 5.5
10,000	0.25	17.0	〃	2.5 x 5.5
30,000	0.25	40.0	4 or more	3.3 x 6.5
50,000	0.20	48.0	〃	3.3 x 6.5
100,000	0.15	54.0	〃	3.3 x 6.5
150,000	0.15	71.0	5 or more	3.3 x 6.5
200,000	0.15	93.0	〃	3.3 x 6.5
330,000	0.15	155.0	4 or more	4.5 x 9.0
500,000	0.15	231.0	〃	4.5 x 9.0

Figure 4.7: Fender Selection Quick Reference Guide [57]

Table 4.3: Shuttle Tanker Specifications [59]

Parameter	**Value**
Classification	Shuttle Tanker
Length Overall (m)	282
Beam (m)	49
Deadweight (tonnes)	153,684
Displacement (tonnes) [1]	200,000

Once moored, a crane-supported gangway is positioned directly between the platform and the shuttle tanker and secured at both ends. The design of the enclosed gangway is pivotal for the secure at-sea transport of fuel pebbles. It draws inspiration from modular gangways designed for marine conditions, such as those manufactured by Tyne Gangway, as depicted in Figure 4.8a. Nevertheless, due to the shielding requirements highlighted in Chapter 5 section 5.6, the traditional aluminum construction is replaced with carbon steel. This material is chosen for its durability, strength, cost-effectiveness, and established usage in nuclear ship design. Carbon steel also provides some corrosion resistance and weldability. While concrete offers lower weight and cost, it has a lower electron density, making it less effective at shielding against gamma radiation compared to steel. A complete shielding evaluation, detailed in Section 5.6, determines that 4 cm of lead is necessary to achieve the required attenuation. Comparisons of steel and concrete's shielding capabilities are presented in Table 4.4, leading to the selection of carbon steel for the gangway's shielding.

Two high-pressure stainless steel hoses, each 0.20 m in diameter—three times the diameter of the fuel pebbles recommended for dilute phase pneumatic systems—and 4 meters in length, are thoughtfully installed on a track within the gangway [60]. These hoses are used to provide a dual-path system, where the presence of the second hose serves as a redundancy measure. This setup is inspired by the hose systems used in underway replenishments, where the redundancy is essential for maintaining operations despite the harsh marine environment. As depicted in Figures 4.8, the primary hose connects the platform's nitrogen supply line to the onboard conveying pipeline via quick connect/disconnect couplings, enabling the efficient pneumatic conveyance of 0.06 m diameter fuel pebbles from the storage tank, propelled by an upstream turbo-compressor through the gangway. The second hose stands ready to take over or supplement the pebble transfer should the first encounter any operational issues, thus ensuring uninterrupted service and enhancing safety. The pebbles are then directed into the shuttle tanker's pneumatic system, and subsequently into onboard holding tanks for temporary storage before their eventual placement into canisters and casks within the tanker. This dual-hose configuration not only maximizes the safety and reliability of the transfer process but also reflects advanced naval replenishment techniques adapted for nuclear material handling.

[1] Estimated value based on typical ship design proportions.

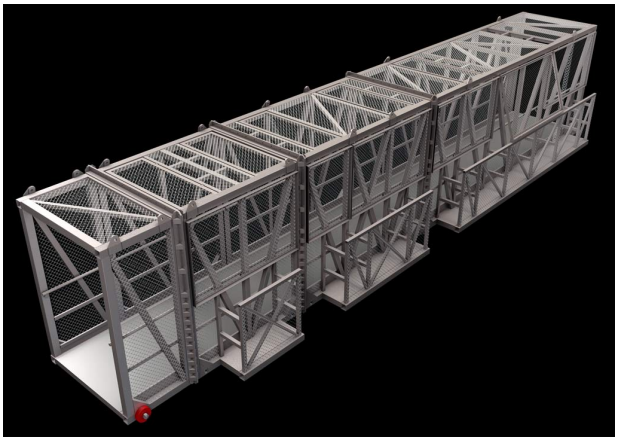

(a) Perspective View Modular Gangway[61]

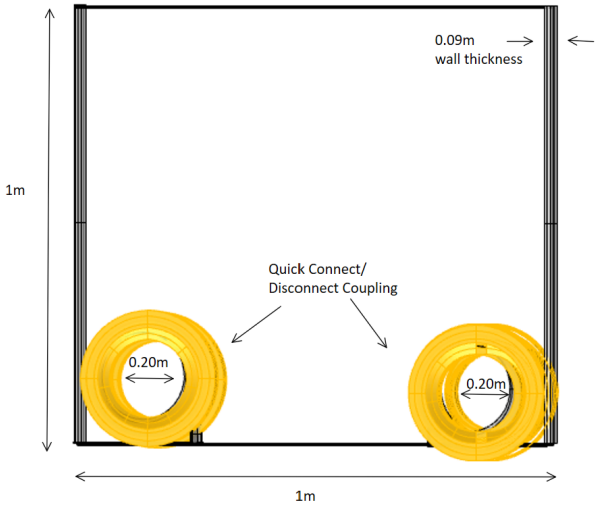

(b) Front View Parallel Hoses in Gangway

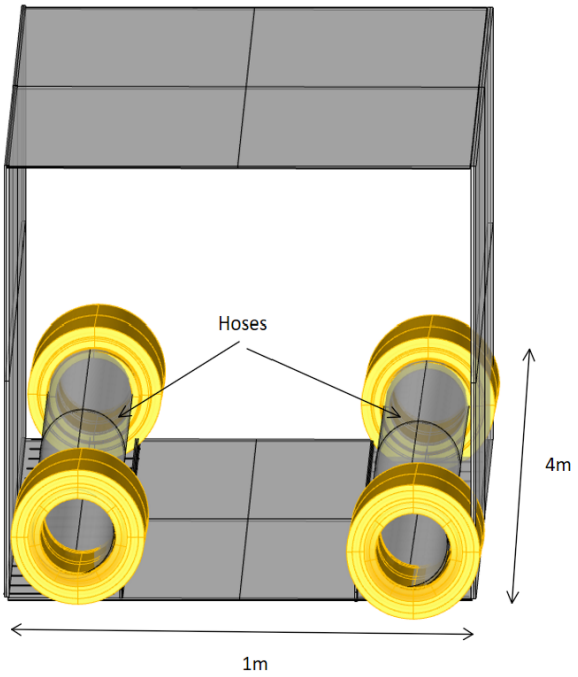

(c) Tilted Front View of Parallel Hoses in Gangway

Figure 4.8: Various views of the Enlosed Gangway and the parallel hoses used for pebble transport.

Pneumatic Conveyor System Overview The pneumatic conveyor system operates on the dilute phase principle, ideal for transporting materials like fuel pebbles that are suspended in a pressurized nitrogen gas stream. Nitrogen is preferred over air, which can introduce oxidation risks and potential hydrogen generation, and helium, which would require higher pressures due to its lower density, thus increasing operational costs. The chosen pos-

itive pressure system offers material compatibility, extending established handling practices from reactor operations, and ensures operational control remains with the OFNP, enhancing reliability and independence from the receiving ship's conditions.

Operational Control and Monitoring During operation, the flow of fuel pebbles and nitrogen gas is continuously monitored and controlled to maximize safety and efficiency. The system's design minimizes component wear, accommodating the discharge of 0.06 m fuel pebbles from the holding tank. The pebbles travel at a speed of 10.6 m/s, propelled by nitrogen supplied upstream at 1.034×10^6 Pa and at a velocity of 12.6 m/s. They move through a quick connect coupling and a 0.20 m diameter, 4 m long hose that resides within the enclosed carbon steel gangway. At the output end, the hose connects to the shuttle tanker, which receives the fuel pebbles and directs them into a holding tank before they are transferred to canisters and casks. To control the velocity at which the fuel pebbles enter the holding tank, thereby preventing damage, the nitrogen supply pressure can be adjusted. Lowering the nitrogen pressure reduces the pebbles' propulsion speed, allowing for a softer landing into the holding tank. Additionally, the system can be equipped with variable-speed controls for the nitrogen supply, allowing the flow rate to be adjusted as needed. This flow path is illustrated in Figure 4.9. Flow and pressure sensors are distributed throughout to permit early detection of any stuck fuel pebbles, or hose ruptures requiring action to be taken.

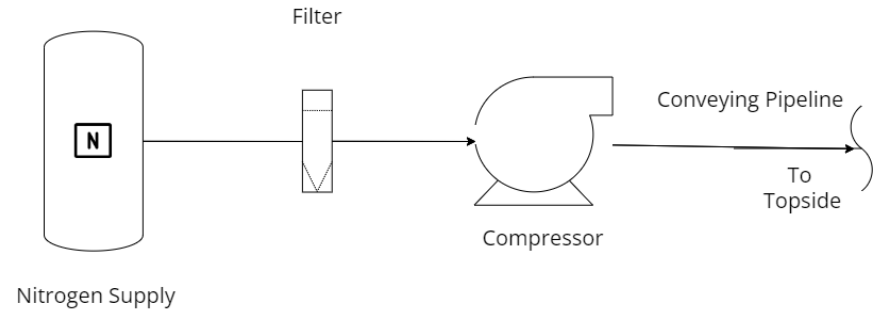

(a) Pneumatic Supply Room

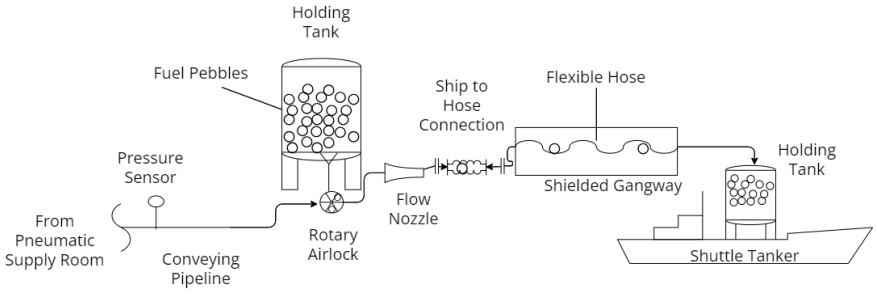

(b) Topside Configuration

Figure 4.9: One Line Diagram of Pneumatic System

Table 4.4: Gangway Design Specifications and Cost Comparison for Different Materials [62],[63],[64]

Parameter	**Lead**	**Steel**	**Concrete**
Material Density (kg/m^3)	11,350	7,800	2,300
Thickness (m)	0.04	0.09	0.27
Gangway Volume (m^3)	0.88	1.86	4.47
Estimated Mass of Gangway (kg)	9,976	14,508	10,281
Total Material Cost (USD) [1]	$ 21,300	$ 1,500	$ 900

Key considerations for this design also include the system's temperature and pressure limitations, which are analyzed against the calculated flow rate and pressure drop discussed below to ensure optimal operation. The specifications and operational parameters of the pneumatic system are summarized in Table 4.5.

Table 4.5: Pneumatic System Specifications [65]

Parameter	**Value**
Minimum Conveying Fluid	Nitrogen
Minimum Conveying Velocity (m/s)	12.7
Fluid Temperature $^\circ C$	25
Pressure (Pa)	1.034×10^6
Pebble Velocity (m/s)	10.16
Hose Maximum Temperature $^\circ C$	815
Hose Maximum Pressure (Pa)	3.792×10^6
Hose Material	316SL
Hose Length (m)	4
Hose Inner Diameter (m)	0.10
Hose Outer Diameter (m)	0.13
Hose Weight (kg)	35.70

Flow Rate Calculation The conveying velocity (v) for the pneumatic system was set at 12.7 m/s, a value within the typical range for dilute phase pneumatic conveying systems [66]. This velocity falls within recommended dilute phase velocities for bulk materials of a similar size and density as the fuel pebbles allowing the fuel pebbles remains suspended in the conveying medium, as defined as a dilute phase system.

The expected volumetric flow rate through the hose was determined using equation 4.2 [67],

$$Q = A \cdot v \approx 1480(\text{m}^3/\text{h}) \tag{4.2}$$

where Q is the volumetric flow rate, A is the cross-sectional area of the hose, and v is the velocity of the gas stream carrying the fuel pebbles.

[1] Estimated cost of required materials.

Total Pressure Drop The total pressure drop in the system was calculated as [66]:

$$\Delta P_T = \Delta P_{acc} + \Delta P_g + \Delta P_s \approx 371,900 \text{ Pa} \tag{4.3}$$

where

$$\begin{aligned} \Delta P_{\text{acc}} &= \text{Pressure loss due to acceleration of the solids} \\ \Delta P_g &= \text{Frictional pressure loss of the gas} \\ \Delta P_s &= \text{Frictional pressure loss of the solids} \end{aligned}$$

with full pressure drop calculations found in Appendix A 7.2

Compressor System Specifications Upon completing the initial calculations above, Atlas Standardized Centrifugal compressor as shown in Figure 4.10 was used as an example for pneumatic operations. Table 4.6 provides its requisite specifications. [68].

Figure 4.10: Standardized Centrifugal Compressor [69]

Table 4.6: Specifications of the Compressor System [68]

Parameter	**Value**
Effective Inlet Flow (m^3/h)	250 to 110,000
Max Suction and Discharge Pressure (Pa)	7×10^6 Pa

Volumetric Flow Rate Compatibility The system's required volumetric flow rate of 1486 (m^3/h) fell within the operating range of the SC tubocompressor, capable of handling a flow between 250 and 110,000 (m^3/h).

Pressure Drop Compatibility The SC Turbocompressor has a maximum discharge capacity of 7×10^6 Pa. Given its capability, it can manage a pressure drop of 3.7×10^5 Pa. Starting from the atmospheric inlet pressure (1×10^6 Pa), the compressor's discharge pressure exceeds the combined pressure drop and inlet pressure, totaling 6.6×10^5 Pa. Thus, accommodating the system's pressure drop.

4.3.5 Spent Fuel Capture

In response to the potential inadvertent release of spent fuel pebbles during transfer operations, a safety net system is implemented beneath the enclosed gangway. This system is designed to capture any released pebbles, thus mitigating the risk of environmental contamination. An example of a stainless steel mesh net is depicted in Figure 4.11. The specifications for the safety net, needed for the concept design, are based on the net's dimensions, (4.27×1.22) meters, and are compared against various configurations of mesh sizes and cable diameters to ensure flexibility in the net while also preventing the release of fuel pebbles through the mesh. The comparative analysis is detailed in Table 4.7 and the resulting net for the concept design are highlighted in red with a 0.10 meter mesh size, 0.003 meter cable diameter.

In addition to the net, the design also requires that sandbags be positioned inside the net due to absorb the kinetic energy of falling pebbles and to ensure they don't fall through the mesh, ensuring a controlled and secure landing. This dual approach not only captures pebbles effectively but also prevents their potential introduction into the marine environment.

Table 4.7: Safety Net Specifications [70]

Parameter	**Value**
Material	AISI SL 316
Max Temperature $°C$	500

Figure 4.11: Example of Stainless Steel Mesh Safety Net. [70]

Spent Fuel Safety Net Failure In the event of enclosed gangway failure, Equation 4.4 [71] is utilized to quantify the potential energy (PE) of the hose and the gangway when

positioned at an assumed 1m height (h) above the net. Here, m represents the mass of the hose or the gangway, and g is the acceleration due to gravity. For the purposes of the analysis, the potential energy of these structures at the operating height provides an estimate of the kinetic energy in the event of a fall.

$$PE = m \cdot g \cdot h \tag{4.4}$$

The kinetic energy of the fuel pebbles, however, is calculated directly from their motion using Equation 4.5 [71], where (v) represents the velocity of the pebbles. The equation gives the kinetic energy just at the point of system failure.

$$KE = \frac{1}{2}mv^2 \tag{4.5}$$

The calculated energies are as follows:

- Gangway: 97.86 kJ
- Hose: 0.35 kJ
- Fuel Pebbles: 0.42 kJ

Given the cumulative kinetic energy of the falling objects at approximately 98.63 kJ, along with their total mass of 10, 100 kg, the primary concern is the capability of the capture net to effectively catch and begin to decelerate these objects without surpassing its structural limits. The capture net, boasting a SWL of 53, 900 kg, is engineered to withstand the immediate physical impact of the falling objects. This capacity, quantified in terms of mass, offers a substantial margin of safety for capturing and initially decelerating the objects, given the total mass and the kinetic energies involved. The pneumatic fenders, with an energy absorption capacity of 4, 281 kJ, significantly exceed the kinetic energy of the impact, ensuring that the energy is absorbed effectively after the initial catch by the net.

Cable Diameter(m) (SWL per Cable)	**Mesh Size (m)**	**Cables Required**	**SWL (kg)**
0.003 (154.22 kg)	0.10	350	53,900
0.003 (154.22 kg)	0.20	161	24,800
0.003 (154.22 kg)	0.30	90	13,800
0.004 (380.95 kg)	0.10	350	133,300
0.004 (380.95 kg)	0.20	161	61,300
0.004 (380.95 kg)	0.30	90	34,200
0.006 (634.92 kg)	0.10	350	222,200
0.006 (634.92 kg)	0.20	161	102,200
0.006 (634.92 kg)	0.30	90	57,100

Table 4.8: SWL based on Cable Diameter and Mesh Size [72]

4.3.6 Mitigation of Risks

Despite design considerations mentioned above for the at-sea transport system, operational risks remain. This section addresses the measures implemented to mitigate potential failures across system components, These measures are meant to maintain continuous operation and safeguard the environment and personnel involved in the transport process. The following outlines the strategies employed to manage risks associated with critical parts of the system:

- Elevator Failure: To ensure redundancy and enhance reliability, an additional elevator is implemented on both sides of the platform. Both elevators are equipped with mechanical overrides and manual operation capabilities, allowing for continued operation and safe handling in the event of a failure.
- Hose Failure: Sensors are delibertely placed upstream of the hose to monitor the differential pressure of the nitrogen supply. This setup enables early detection of anomalies such as pressure drops or blockages, indicative of potential hose failure. A back flush system is available to clear any detected blockages, and quick disconnect features at both hose ends ensure swift isolation and containment.
- Pneumatic Supply Failure: Redundant compressors are installed, each capable of independently supporting the system's full operational demands. This redundancy ensures that the system can maintain operational integrity and continuity, even in the event of a failure in one of the pneumatic supply sources.

4.4 Defueling the Reactor

To ensure the successful defueling of the reactor at the end of its operational life, it is essential to identify suitable harbors that can service the OFNP and to determine the appropriate methodologies for transporting the platform. These steps are important because the selected harbor must not only meet the specific requirements of the OFNP but also support the chosen transport methods, whether involving heavy lift ships or tugs. This process works in conjunction with efforts to safely bring the platform into the shipyard. Once in the shipyard, the remaining fuel is to be removed from the platform in accordance with safety regulations.

4.4.1 Harbor Port Selection

The evaluation of suitable harbor ports is conducted based on depth restrictions to accommodate the platform. An assessment identifies the top ten deepest harbor ports worldwide, taking into account their maximum depth capabilities, which range from 16 to 28 meters as shown in 4.9.

4.4.2 Adjustment of Full Load Displacement

Concurrently with identifying an appropriate harbor, strategies are developed to reduce the OFNP's full load displacement to its lightship displacement, defined as the displacement

Table 4.9: Deepest Sea Ports in the World [73]

Port Name	Location	Maximum Depth (meters)
Port of Sines	Portugal	28
Yangshan Port	China	27
Port of Rotterdam	Netherlands	24
Port of Tanger Med	Morocco	22
Europort	Netherlands	24
Port Hedland	Australia	20
Port of Santos	Brazil	17
Busan Port	South Korea	17
Colombo International Container Terminal	Sri Lanka	18
Port of Hamburg	Germany	16

of the ship when it is without any ballast water, fuel, or stored pebbles. The platform is designed to store up to five years' worth of spent fuel, equating to 40 canisters, each capable of holding 40,000 pebbles. Considering the mass of one pebble at 0.2 kg and the empty mass of each canister at 6 tonnes, calculations are performed to determine the total mass of the canisters. Additionally, the removal of transport casks, each with an empty mass of 76.5 tonnes, is evaluated. However, even with the removal of all casks, the platform's weight is only reduced by 3060 tonnes.

Furthermore, the platform's adjustable ballast systems are evaluated for their potential in deballasting. The platform features an adjustable ballast system at and double hull, along with a flooded hull and flooded skirt. The masses of these ballast systems are detailed in Appendix 7.1. Their removal allows for a reduction in draft to approximately 24 meters, a draft that is viable for some of the world's seaports.

The following table outlines the OFNP's displacement characteristics and ballast masses:

Table 4.10: Adjustment of Full Load Displacement

Parameter	Mass (tonnes)	Draft (meters)
Total Mass of 5 Years' Fuel Onboard	292	-
Total Mass of 5 Years' Canisters (40 units)	240	-
Total Mass of 5 Years' Casks (40 units)	3060	-
Total Mass of Ballast Tanks	168596	-
Total Mass of Ballast Systems	236484	-
Full Load Displacement	380166	77
Lightship Displacement	141142	24

4.5 Platform Transportation

The methodologies for relocating the platform from the open ocean to drydock are discussed in this section Focusing on the use of heavy lift ships and tugs, and addressing the navigational assessments necessary to ensure safe passage.

4.5.1 Transportation by Tugs

Primarily, tugs provide a more maneuverable means to transport the OFNP, particularly useful in narrower waterways or where precise control is necessary:

- **Positioning and Towage:** Coordination of the towage process aligns with harbor approaches and dock placements.
- **Clearance Assessments:** Survey of the intended route ensures clearance from bridges, overhead structures, and canal thresholds, particularly noting areas where the vertical clearance is less than 84 meters as potential constraints.

4.5.2 Transportation by Heavy Lift Ship

Alternatively, heavy lift ships, designed to carry massive loads like the Dockwise Vanguard, at 117,000 tonnes, could be a method for transporting the platform to a defueling location. This approach requires either a reduction in the OFNP lightship displacement from 148,000 tonnes to 117,000 or the construction of a new heavy lift ship that can withstand the OFNP displacement. In the event a heavy lift ship is to be used, the following must be considered:

- **Load Management:** Adjusting the platform's height and positioning on the heavy lift ship to manage the overall submergence based on the ship's loading specifications.
- **Navigational Clearances:** Ensuring that the total height of the OFNP aboard the ship does not surpass limits set by bridge and overhead cable clearances along the transport route.
- **Draft Restrictions:** Matching the draft of the fully loaded ship with depth limitations of harbors and canals, ensuring the ship can navigate without grounding.

4.5.3 Clearance and Navigational Considerations

Regardless of the chosen method, the transition of the OFNP into a drydock or pier necessitates navigational planning to mitigate risks associated with vertical clearances and harbor infrastructure:

- **Bridge and Overhead Obstructions:** Identification of potential obstacles along the transit route that may impede safe passage.
- **Tidal Influences:** Utilization of tidal data to time the transport operations, optimizing for periods of maximum water depth to enhance safety margins under overhead constraints.

Chapter 5

Feasibility Analysis

5.1 Introduction

This chapter delves into the comprehensive analysis conducted to validate the feasibility of the OFNP. It reviews the arrangements to ensure that all equipment and rooms onboard are appropriately stored within the confines of the OFNP. This encompasses the entire fuel handling and transport design, which includes storage, at-sea transfer while the platform is moored, and the defueling process which necessitates unmoorinng and relocating the platform to a drydock for maintenance.

Given the nature of these operations, the analysis also assesses the stability and seakeeping abilities of the platform to ensure it remains upright when unmoored from the seabed, so that it can be brought pierside via tugs or heavy lift ship. Furthermore, the introduction of an enclosed gangway structure, for at-sea offloading tasks is evaluated to confirm its structural integrity under the load of passing fuel pebbles, ensuring it does not buckle under the weight.

5.2 Arrangements

The OFNP arrangement facilitates the storage and transport of spent fuel pebbles using heavy-duty bucket elevators. Cranes positioned atop the platform handle the enclosed gangway for secure at-sea transfers. A safe room above the control room limits personnel exposure to fuel pebbles during transfers as shown in Figures 5.1 and 5.2. Figures 5.3 depict the platform in its STS configuration, illustrating the operational setup for at-sea transfers.

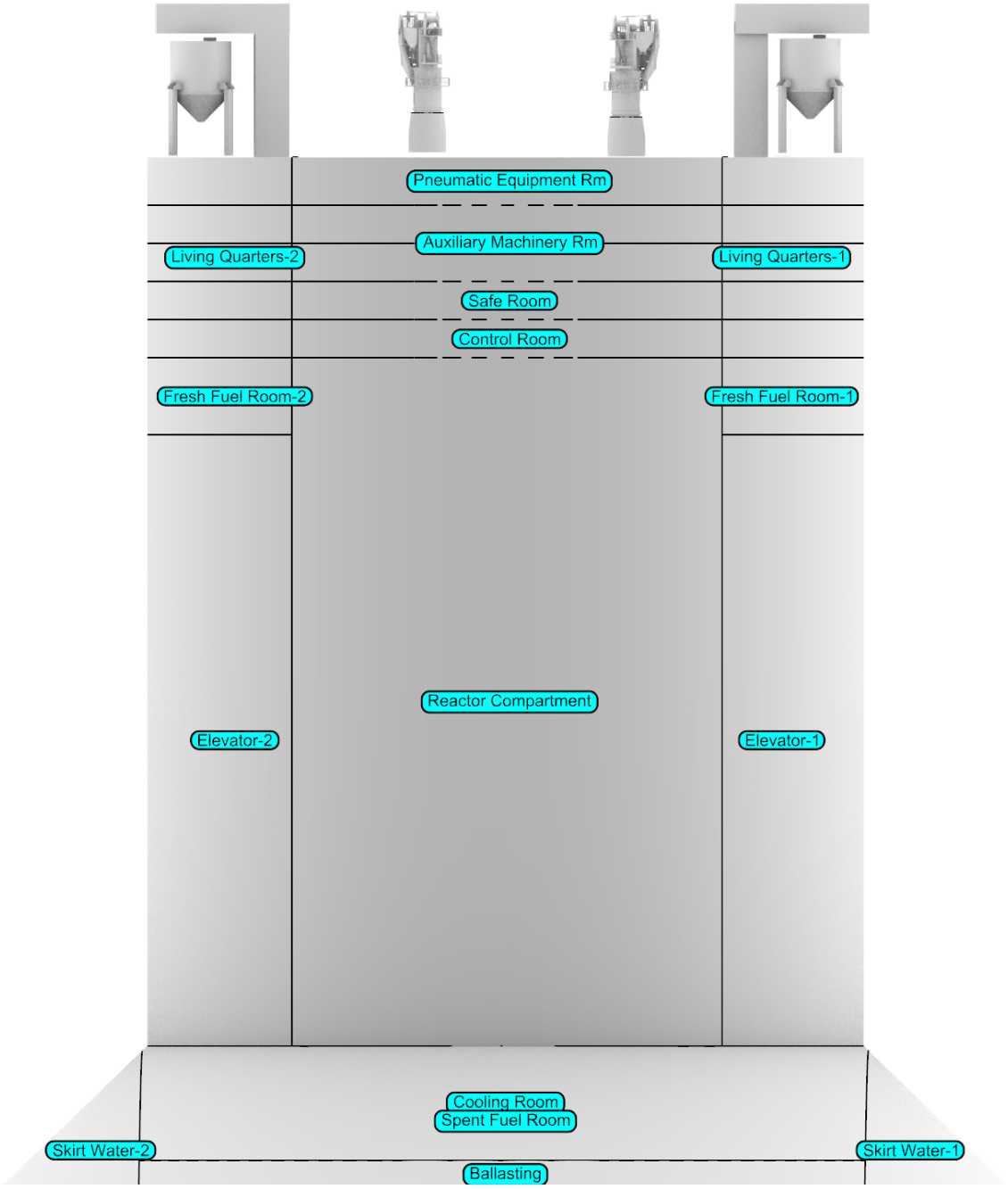

Figure 5.1: Front View of Platform

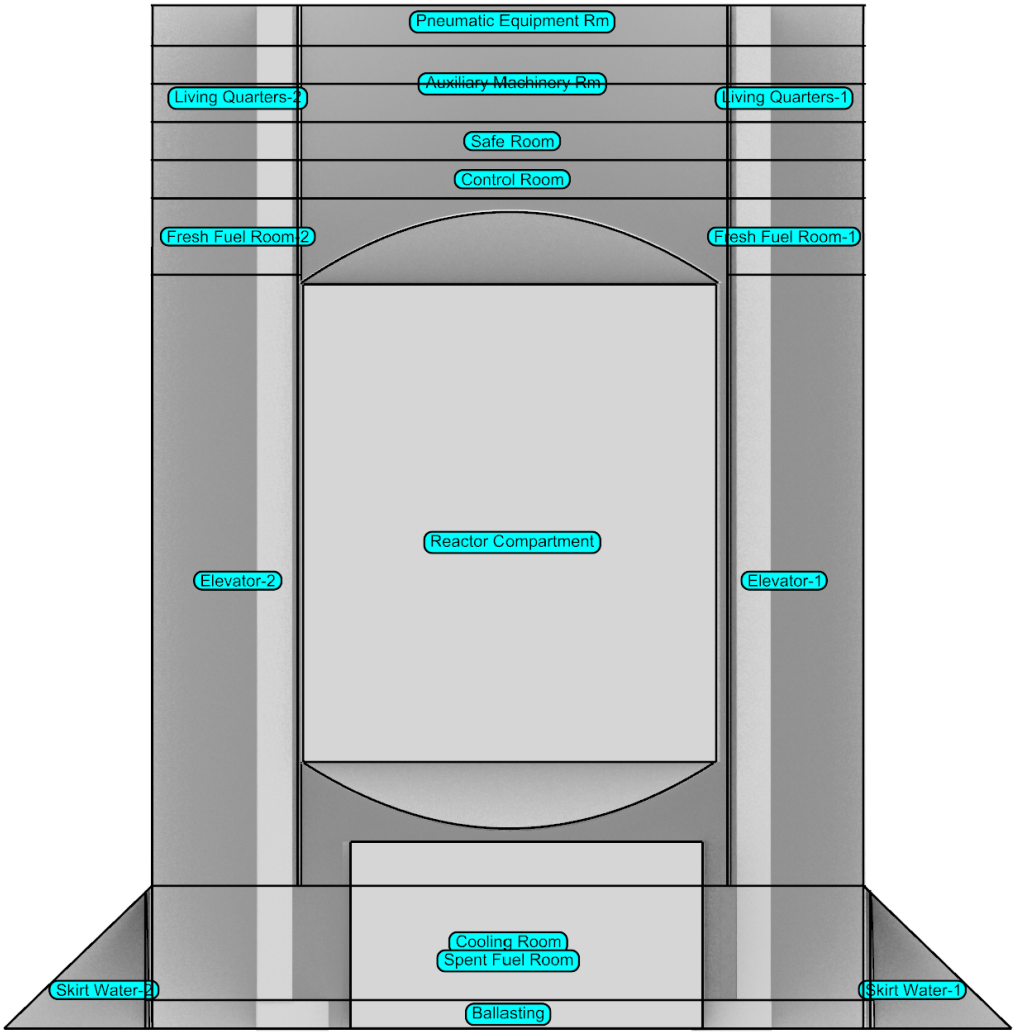

Figure 5.2: Clipped Front View of Platform

(a) Rendered Top Side View of Platform in STS Configuration

(b) Rendered Perspective View of Platform in STS Configuration

Figure 5.3: Different Rendered Views of the Platform in STS Configuration

5.3 Stability Analysis

A equilibrium stability analysis is conducted using Marine Vessel Analysis And Design Software (MAXSURF), a software suite from Bentley Systems, designed to support naval architects and shipbuilders. This suite provides a set of tools for hull form modeling, hydrostatic and stability calculations, performance analysis, and structural assessment, facilitating an integrated approach to modern ship design and analysis.

This analysis is based on the Mass Distribution outlined in Appendix 7.1. The mass distribution table, adapted from prior OFNP designs, has been modified to reflect the characteristics of a PBR rather than the previously evaluated PWR [9]. The adjusted mass distribution influences the center of gravity, which is a determinant of the platform's stability.

The results showcased in the Table 5.1 are indicative of the platform's stability. The displacement is significant, suggesting a well-balanced structure that contributes positively to static stability. The draft amidships, being substantial, suggests a low and favorable center of gravity that aids in the platform's buoyancy and stability. Furthermore, the corrected Transverse Metacentric Height due to Gravity (GM) defines a significant righting moment, confirming the vessel's strong transverse stability and its capacity to resist rolling in adverse sea conditions.

The slight positive trim, quantified in both meters and degrees, demonstrates a design that optimizes the hydrodynamic profile without sacrificing stability. Together, these findings, derived from MAXSURF, not only validate the design's practicality when defueling occurs.

Table 5.1: Equilibrium Stability Parameters

Parameter	**Value**
Displacement (tonnes)	380,166
Draft Amidships (m)	76.99
GMt (m)	9.50
Trim (+ve) (m)	0.299
Trim Angle (+ve) (deg)	0.23

International Maritime Organization (IMO) Criteria

The intact stability criteria assessment, summarized in the table, validates the seaworthiness and safety of the OFNP. Each criterion is carefully measured against standards set by the IMO, which is the global authority responsible for regulating shipping. In particular, they specify criteria as described below for offshore supply vessels and rigs much like the OFNP. The IMO's rules ensure that ships are constructed to be safe, environmentally sound, and designed to prevent maritime accidents.

- Righting Arm (GZ) area: results signifies the ship's ability to right itself after being tilted, a key factor in preventing capsizing i.e. righting arm. The OFNP figure vastly

exceeds the IMO's required standard, highlighting an exceptionally stable vessel right from the start.

- Area between 30 to 40 degrees: indicates the vessel's capacity to recover from substantial tilting. Surpassing the required area significantly, the OFNP demonstrates strong stability, even in turbulent conditions.
- Maximum GZ: reflects the peak righting leverage of the vessel—a higher value means the ship can effectively counteract heeling. Here, the actual value greatly exceeds the minimum standard, ensuring the vessel's tenacity in returning to an upright position.
- Angle of Maximum GZ: is the point where the vessel's righting leverage is strongest. The much higher actual angle compared to the standard requirement implies that the OFNP can sustain stability over a broad range of tilting angles, enhancing safety.
- Initial GM: measures the vessel's resistance to rolling motions. Exceeding the IMO standard by a wide margin, the OFNP showcases stability, crucial for maintaining balance while preparing to be unmoored.

Table 5.2: Intact Stability Criteria Assessment Results

Criteria	**Value**	**Units**	**Actual**	**Status**
GZ area between 0 and angle of max GZ	3.15	m.deg	698.05	Pass
Area 30 to 40	1.72	m.deg	57.79	Pass
Maximum GZ at 30 or greater	0.20	m	19.48	Pass
Angle of maximum GZ	15.0	deg	85.0	Pass
Initial GMt	0.15	m	9.01	Pass

5.4 Seakeeping

The seakeeping capabilities of the platform are analyzed using MAXSURF Motions, a program within the Bentley Systems designed to assess a vessel's performance on the water. Seakeeping specifically refers to how well a ship or platform maintains its effectiveness and safety in the marine environment, especially in the face of wave-induced movements such as roll, pitch, and yaw. These responses impact the platform's operational stability and the well-being of its crew and equipment.

The platform's symmetrical design plays a significant role in its seakeeping properties, leading to similar behavior patterns in roll and pitch motions according to the analysis. This symmetry is advantageous in maintaining balance and stability, providing predictable responses to oceanic forces.

The analysis operates under the assumption that the highest sea state the platform will encounter during the preparatory decommissioning phase is sea state 4. This moderate condition, characterized by significant wave heights up to 2.5 meters, is the upper limit for the platform to be unmoored safely. Additionally, during such operations fuel transfer

is halted if wind and current exceed 25 and 5 knots respectively [74]. This conservative approach ensures that the platform avoids excessive roll, pitch, and yaw motions, which are important for maintaining operational safety and structural integrity.

MAXSURF Motions furnishes a visual account of the platform's behavior in response to these sea conditions. The results, displayed in Figure 5.4 demonstrate that the platform's roll and pitch movements are restrained to less than 1 degree even in sea state 4, substantiating the design's efficacy in preserving stability. This level of motion control is vital for ensuring the safety and success of decommissioning operations, safeguarding against mishaps, and protecting the platform's structure and onboard systems.

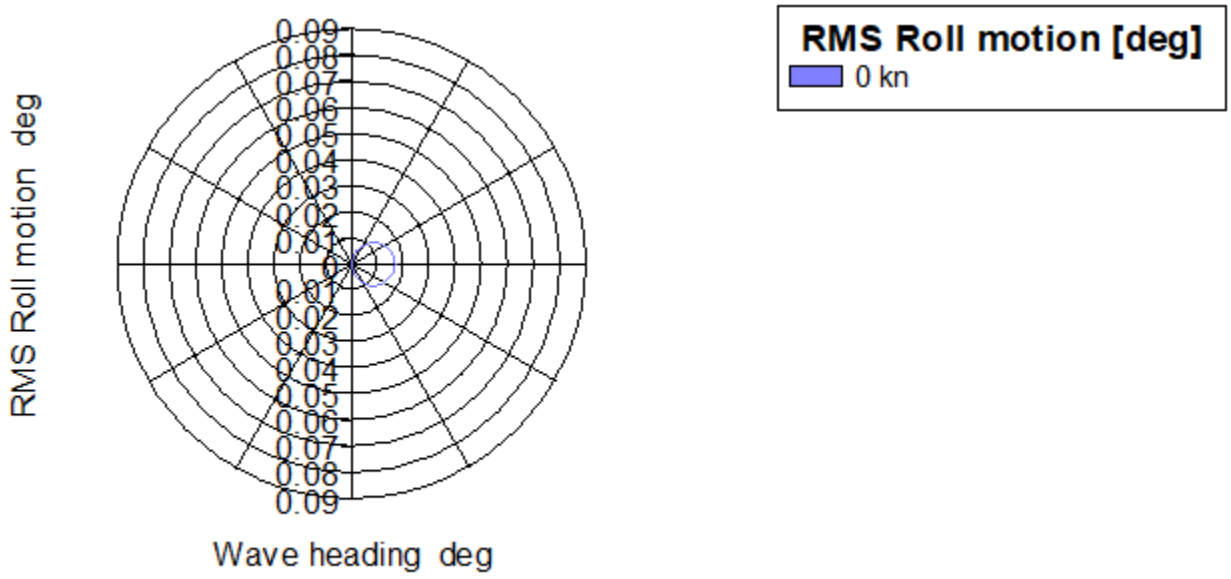

Figure 5.4: Sea State 4 Roll/Pitch Motion

5.5 Structural Analysis

5.5.1 Enclosed Gangway

To assess the structural integrity of the gangway under load, a static analysis was conducted. The gangway was modeled as a fixed-fixed beam, a configuration chosen due to its secure anchorage at both ends during operation, which prevents any rotation or vertical movement at the supports.

Euler-Bernoulli beam theory, suitable for predicting the behavior of slender beams under various loading conditions, was employed for this analysis [75]. This theory helps calculate the maximum deflection of a beam subjected to uniformly distributed loads, such as the continuous weight of fuel pebbles moving through a hose. Using these equations provides a conservative estimate of deflection, ensuring that the gangway's design incorporates adequate safety margins for the expected loads. The chosen material for the gangway, stainless

steel, not only provides the necessary strength to support these loads but also serves as a containment barrier for safely transferring individual fuel pebbles.

The application of these principles ensures that the gangway maintains its structural integrity by preventing excessive deflection, thus guaranteeing the safety and efficiency of the operation. The calculations and resulting data from this analysis are detailed in Figure 5.5, demonstrating the gangway's capability to withstand the demands of fuel transfer.

$$\text{Bending Moment Calculation: } M(x) = \frac{w}{2}x(L-x) \tag{5.1}$$

$$\text{Deflection Calculation: } \delta(x) = \frac{wx(L^3 - 2Lx^2 + x^3)}{24EI} \tag{5.2}$$

$$\text{Stress: } \sigma(x) = \frac{M(x) \cdot y}{I} \tag{5.3}$$

$$\text{Shear: } V(x) = w(\frac{L}{2} - x) \tag{5.4}$$

$$\tag{5.5}$$

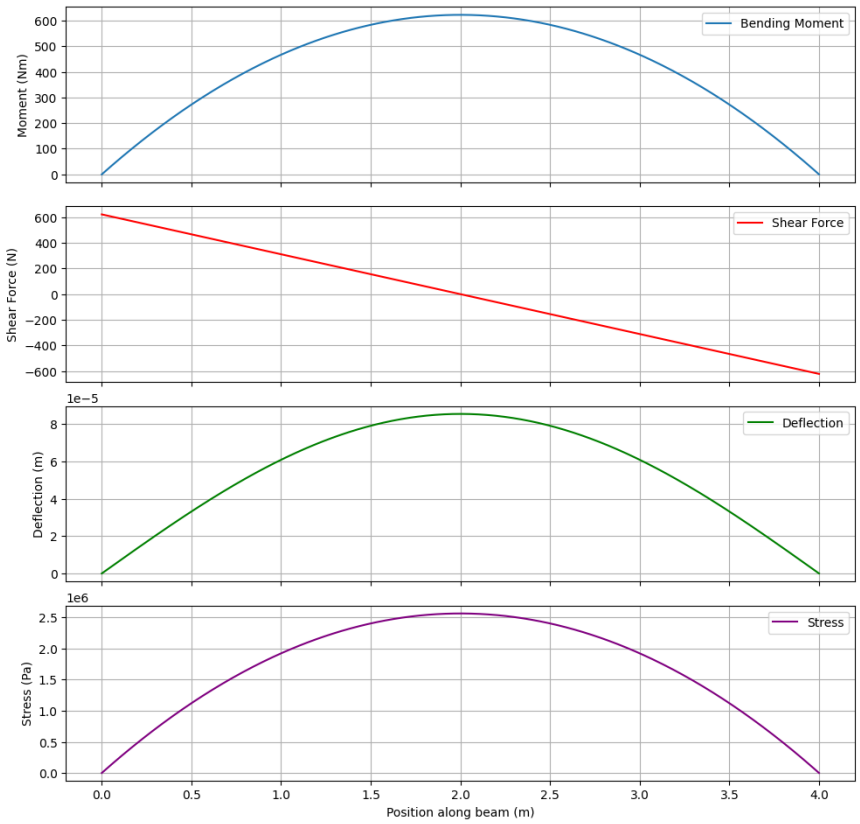

Figure 5.5: Shielded Gangway Structural Analysis [76]

Max deflection : 8×10^{-5} m

Peak stress : 2.5×10^{6} Pa

Comparing the results to the material specifications in Table 5.3, gangways' stress under load did not exceed yield strength of material at 0.45% yield strength.

Table 5.3: Gangway Material Specifications [77]

Parameter	**Value**
Tensile Strength (MPa)	795
Yield Strength (MPa)	550
Young Modulus (GPa)	200

5.6 Shielding

5.6.1 Introduction

In designing the fuel transport system for the OFNP, a primary objective is to ensure radiation exposure to personnel is minimized, particularly in scenarios that could lead to prolonged exposure, such as equipment malfunction. This analysis evaluates suitable shielding materials and their requisite thicknesses, drawing from the findings of prior research on the HTR-PM fuel transport pipeline. That study utilized the QAD-CGA program for efficient dose calculations in simple geometries and considered both spent and partially spent fuel elements [78].

This study's relevance is its examination of 60mm spherical fuel elements—identical to those planned for the OFNP—over a 40-year operational life. It provided insights into the initial dose rates for a 5m stainless steel pipeline, as measured at a 30 cm distance, and investigated the dose rate variations across a range of pipeline lengths and distances from the source.

5.6.2 Hose and Gangway Shielding Analysis

The shielding assessment for the OFNP uses the referenced study's results for a 4m pipeline as listed in Table 5.4, to inform the shielding requirements for a 4m stainless steel hose. This hose is part of a gangway system that serves as the initial radiation barrier. The study's findings, particularly for the unshielded and 4cm lead-shielded scenarios, have been instrumental in shaping the OFNP's design to ensure radiation exposure remains within safe limits.

An integral component of the shielding strategy is the use of steel or concrete as alternatives to lead. This decision was informed by an evaluation of Half Value Thickness (HVT) for various materials, as shown in the following table:

Table 5.4: Dose rate ($\dot{D}$) of hose from source term

Pipeline length (m)	$\dot{D}$ (mGy/h)	
	With no shielding	4 cm lead shielding
4	314	2.86

Table 5.5: Comparison of required shield thickness for Lead, Steel, and Concrete based on HVT values.

Material	**HVT (cm)**	**Required Thickness (cm)**
Lead	0.7	4
Steel	1.6	9.14
Concrete	4.8	27.41

The HVT values guide the determination of how much material is needed to attenuate radiation to the same degree as the lead shielding used in the study. By applying these HVT values, we calculate that 9.14 cm of steel or 27.41cm of concrete would provide attenuation equivalent to 4cm of lead. These material thicknesses were assumed for the OFNP design, ensuring a cost-effective yet safe shielding solution.

5.6.3 Bucket Elevator Shielding Analysis

The shielding analysis for the bucket elevator differs from the hose due to its rectangular geometry, making direct application of studies based on pipe geometries unreliable. Nonetheless, the source strength S is assumed constant across different configurations, which aids in generalizing the analysis.

Using the following equation to back-solve for S [79]:

$$\dot{D} = \frac{S}{4\pi r^2} \tag{5.6}$$

where:

$$\begin{aligned} D &= \text{Dose rate (mGy/h)}, \\ S &= \text{Source strength (mGy} \cdot \text{cm}^2\text{/h)}, \\ r &= \text{Distance from source (cm)}. \end{aligned}$$

Once S is determined, the shielded flux is calculated via [80]:

$$\text{Flux}_{\text{shielded}} = \frac{S}{4\pi r^2} \times e^{-\mu x} \tag{5.7}$$

[0]Specifies the maximum permissible dose rate for personnel in the radiation zone.

where:

$$\begin{aligned} \text{Flux}_{\text{shielded}} &= \text{Shielded flux (Gy/s)}, \\ \mu &= \text{Linear attenuation coefficient (cm}^{-1}\text{)}, \\ x &= \text{Thickness of shielding material (cm)}. \end{aligned}$$

Utilizing steel with a linear attenuation coefficient μ of $0.56\,\text{cm}^{-1}$ [81], and a gamma constant (Γ) assumed to be $0.08\,\text{Gy} \cdot \text{cm}^2 \cdot \text{s}^{-1}$ [82]. The dose rate for the shielded system is then determined by the product of the gamma constant and the shielded flux:

$$\text{Dose Rate}_{\text{shielded}} = \Gamma \times \text{Flux}_{\text{shielded}} \tag{5.8}$$

These calculations facilitate determining dose rates at a 30cm distance from the source for various thicknesses of steel, corresponding to the wall thickness of the bucket elevator. A point source depiction of a stuck bucket elevator and personnel onboard, considering stainless steel wall thickness, is illustrated in Figure 5.6.

Table 5.6: Shielded Dose rate of iron

Thickness (cm)	Dose Rate (mGy/h)
4	24.23
8	2.59

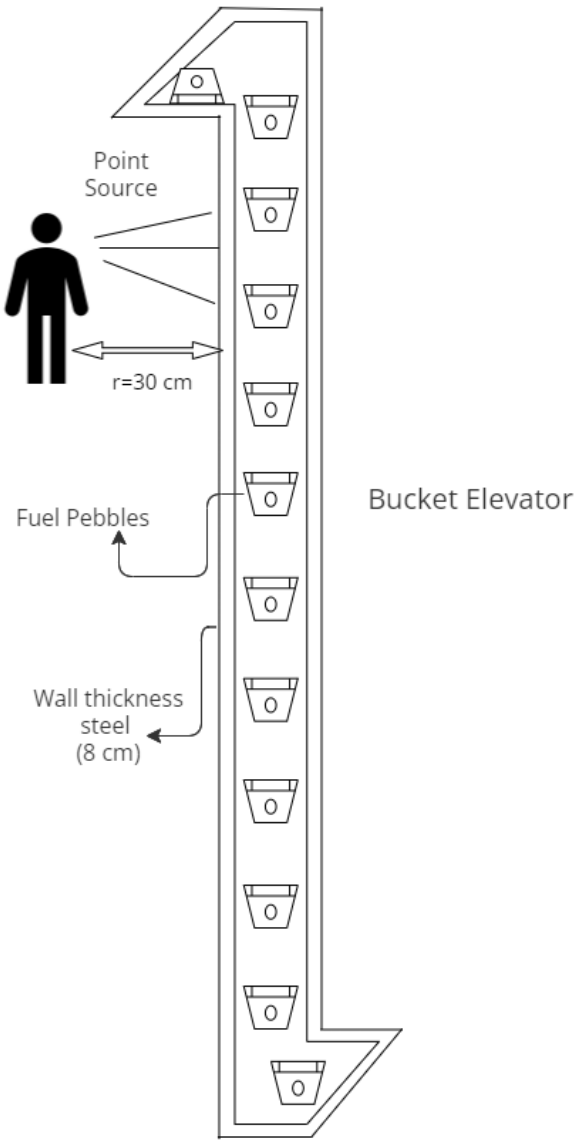

Figure 5.6: Shielding Diagram for Point Source due to Stuck Elevator

Additional Safety Measures: To further mitigate radiation exposure during at-sea fuel transfers, since several assumptions were made in estimating the expected dose rate from the bucket elevator, given it traverses the full length of the platform, distance itself serves as a critical factor in reducing exposure. Thus by placing a safe room in the OFNP 8 meters away from either elevator radiation exposure can be reduced further.

Chapter 6

Future Research and Conclusion

6.1 Future Research

Given the nature of the OFNP's operations, several areas require further investigation to enhance the fuel handling system. A detailed dynamic stability simulations are essential to assess the effects of the platform being moored with fenders, along with evaluating the dynamic response due to the relative motion of the tanker. Additionally, there is a need to expand the shielding analysis beyond a single study to encompass a broader range of materials and configurations, which could help determine the most effective materials for the bucket elevator and the enclosed gangway.

Investigating the functionality of the gangway in more detail, focusing on operational isolation systems that can effectively segregate the gangway from the main platforms in the event of a rupture or other structural failures. Developing emergency response strategies that can be rapidly deployed to isolate and repair compromised sections without jeopardizing the entire system is also vital.

Moreover, using simulation tools to model the at-sea transfer process will help optimize operations under varying environmental conditions and improve safety protocols during critical transfer operations. The integration of robotics to automate the fuel handling process can reduce human exposure and increase operational accuracy. Developing a network of sensors for real-time monitoring of radiation levels, structural health, and system operations will enhance oversight and safety. Finally, designing automated systems that can swiftly isolate parts of the fuel handling system during malfunctions will minimize risks and enhance overall safety.

6.2 Conclusion

In this thesis, we delve into the design and operational challenges of integrating SMR into an offshore setting through the OFNP. This study aligns with global efforts to combat climate change by promoting nuclear energy as a stable, efficient alternative to fossil fuels.

6.2.1 Summary of Findings

We investigate the potential of HTGR, particularly PBR, to safely transport fuel in marine environments. The OFNP's fuel handling, storage, and transfer systems are tailored to meet the unique demands of the offshore environment.

- **Fuel Handling and Storage**: The design of the OFNP includes a fuel handling system that supports at-power fuel replenishment, significantly reducing operational downtimes and boosting fuel cycle efficiency. The horizontal at-sea transport system employs pneumatic transfer of fuel pebbles, demonstrating feasibility for offloading fuel pebbles at sea and minimizing the need for large-volume onboard spent fuel storage.
- **Structural and Stability Analysis**: The analyses verify that the platform upholds structural integrity and stability under diverse maritime conditions, crucial for long-term operational viability. This ensures that the OFNP withstands harsh maritime conditions while meeting safety and performance standards.
- **Feasibility of Offshore Operations**: The operational feasibility of the OFNP is affirmed through qualitative assessments based on mathematical models and a review of open-source literature. These evaluations confirm the platform's capability to function as a reliable power source.

6.2.2 Final Thoughts

The integration of advanced fuel handling and transport systems, drawing from proven technologies such as HTR-PM, underscores the feasibility and necessity of the concept design. By implementing targeted modifications, particularly in the pneumatic transport system and bucket elevator, the OFNP effectively reduces radiation exposure and environmental risks. These systems would utilize automated processes to diminish human interaction with radioactive materials and incorporate advanced shielding and containment strategies that exceed conventional safety standards. These enhancements are not only plausible but essential for maintaining the safety and efficiency of the OFNP's fuel management operations, positioning it as a model for future sustainable nuclear energy solutions.

Chapter 7

Appendix A

7.1 Mass Distribution

Table 7.1: Mass Distribution

Item Name	**Quantity**	**Total Mass (tonne)**	**LCG (m)**	**TCG (m)**	**VCG (m)**
Containment Cradle	1	460.00	0.00	0.00	3.00
CA04 and CB65-66 module	1	100.00	0.00	0.00	6.00
CA05 module	1	100.00	0.00	0.00	7.00
Lower structure	1	22551.00	0.00	0.00	8.00
RPV	2	1400.00	0.00	0.00	20.00
CA01 module	1	610.00	0.00	0.00	20.00
Helium Tank	1	200.00	0.00	0.00	20.00
Steam Generator	1	1464.00	0.00	0.00	26.00
Containment Shell	1	3600.00	0.00	0.00	36.00
Polar Crane	1	500.00	0.00	0.00	56.00
Spent Fuel Room	1	3418.00	0.00	0.00	16.00
Spent Fuel Room	1	3418.00	0.00	0.00	16.00
Spent Fuel Canisters	20	60.00	0.00	0.00	16.00
Spent Fuel Canisters	20	60.00	0.00	0.00	16.00
Spent Fuel Casks	20	765.00	-19.00	0.00	16.00
Spent Fuel Casks	20	765.00	19.00	0.00	16.00
Diesel	1	200.00	0.00	0.00	93.00
Firewater	1	350.00	0.00	0.00	60.00
Condensate Storage Tank	1	1840.00	0.00	0.00	60.00
Turbine	1	1300.00	0.00	0.00	94.00
Generator	1	700.00	0.00	0.00	94.00
MSR	1	1000.00	0.00	0.00	94.00
FWH	1	1800.00	0.00	0.00	94.00
Dearator	1	1500.00	0.00	0.00	95.00

Table 7.1: Mass Distribution

Item Name	**Quantity**	**Total Mass (tonne)**	**LCG (m)**	**TCG (m)**	**VCG (m)**
Transformer	1	2000.00	0.00	0.00	95.00
Condenser	1	3000.00	0.00	0.00	79.00
Outer Hull	1	14424.00	0.00	0.00	40.00
Inner Hull	1	12844.00	0.00	0.00	48.00
Desalination Units	1	24.00	0.00	0.00	70.00
Auxiliary Systems Levels 1-5	1	10500.00	0.00	0.00	82.00
Auxiliary Systems Level 6-22	1	4500.00	0.00	0.00	43.00
Living Quarters	1	4392.00	0.00	0.00	96.00
Helipad	1	100.00	0.00	0.00	106.00
Skirt Water	1	67888.00	0.00	0.00	7.50
Flooded Hull	1	117611.00	0.00	0.00	40.50
Adjustable Ballast Level 6	1	9343.00	0.00	0.00	70.00
Adjustable Ballast Outside Double Hull	1	6606.00	0.00	0.00	85.00
Adjustable Ballast at Keel	1	35036.00	0.00	0.00	9.50
Iron Ore Ballast	1	40633.00	0.00	0.00	2.00
Elevator (Port)	1	15.00	-22.00	-22.00	50.00
Elevator (Stbd)	1	15.00	22.00	22.00	50.00
Enclosed Gangway	1	14.5	-25.00	0.00	108.00
Enclosed Gangway	1	14.5	25.00	0.00	108.00
Telescopic Crane (Port)	1	16.78	-27.00	0.00	108.00
Telescopic Crane (Stbd)	1	16.78	27.00	0.00	108.00
Hopper Tank (Port)	1	6.00	-18.00	0.00	108.00
Hopper Tank (Stbd)	1	6.00	18.00	0.00	108.00
Ground Crane	1	500.00	0.00	0.00	25.00
Ground Crane	1	500.00	0.00	0.00	25.00
Transfer Cask	1	125.00	0.00	19.00	20.00
Transfer Cask	1	125.00	0.00	-19.00	20.00
Fresh Fuel Storage Room	1	100.00	0.00	0.00	70.00
Total Loadcase		380166.56	0.00	0.01	29.79
VCG fluid					29.79

[1]Longitudianl Center of Gravity (LCG): Horizontal distance from the centroid to the Center of Gravity (CG) along the platform's length.
[2]Transverse Center of Gravity (TCG): Horizontal distance from the centroid to the CG across the platform's width.
[3]Vertical Center of Gravity (VCG): Vertical distance from the keel to the CG.

7.2 Full Pressure Drop Calculation

The total pressure loss in the system were calculate using the following equations [66] :

$$\Delta P_T = \Delta P_{acc} + \Delta P_g + \Delta P_s + \Delta H_g + \Delta H_s + \Delta P_{misc} \tag{7.1}$$

where the last three terms are equal to zero based on the assumption their is no change in elevation in the assessed design nor any miscellaneous equipment identified:

$$\Delta H_g = \text{Elevation pressure loss of the gas,} \tag{7.2}$$
$$\Delta H_s = \text{Elevation pressure loss of the solids,} \tag{7.3}$$
$$\Delta P_{\text{misc}} = \text{Pressure losses from miscellaneous equipment.} \tag{7.4}$$

$$\Delta P_T = \Delta P_{acc} + \Delta P_g + \Delta P_s + \cancelto{0}{\Delta H_g} + \cancelto{0}{\Delta H_s} + \cancelto{0}{\Delta P_{misc}} \tag{7.5}$$

Thus the remaining pressure drop is due to:

$$\Delta P_T = \Delta P_{acc} + \Delta P_g + \Delta P_s \approx 371,900 \text{ Pa} \tag{7.6}$$

Pressure Loss Due to Acceleration of the Solids (ΔP_{acc}):

$$\Delta P_{acc} = \frac{W \cdot V_p}{4640} \approx 182,200\,\text{Pa} \tag{7.7}$$

Given:

$W = 17,966\,\text{kg/s-m}^2$ (Solid mass velocity)
$V_g = 12.7\,\text{m/s}$ (Gas velocity)
$V_p = 0.8 \times V_g = 10.6\,\text{m/s}$ (Particle velocity, 0.8 times the gas velocity)

$$\Delta P_g = \frac{4f \cdot L \cdot \rho_g \cdot V_g^2}{9266 \cdot D} \approx 965 \text{ Pa} \tag{7.8}$$

Given:

$L = 12\,\text{Equivalent length of pipeline (m)}$
$\rho_g = 11.26\,\text{Gas density (kg/m}^3\text{)}$
$V_g = 12.7\,\text{Gas velocity (m/s)}$
$D = .20\,\text{Pipe diameter (m)}$

The Fanning friction factor (f) is determined by:

$$f = \frac{0.331}{\left[\log_{10}\left(\frac{\varepsilon}{3.7D} + \frac{7}{R_e}\right)\right]^2} = 0.004 \tag{7.9}$$

Given:

$$\varepsilon = 0.0005, \text{pipe roughness factor}$$

The Reynolds number (R_e) is given by:

$$R_e = \frac{D \cdot V_g \cdot \rho_g}{\mu_g} = 4.09 * 10^5 \tag{7.10}$$

Given:

$$\mu_g = 7.09 * 10^{-}5 \, \text{Gas viscosity (kg/m·s)}$$

Frictional pressure loss of the solids (ΔP_s):

$$\Delta P_s = \Delta P_g \cdot K \cdot R \approx 188,700 \text{ Pa} \tag{7.11}$$

Given:

$$K \approx 1.5, \text{estimated friction multiplier for solids conveyed.}$$
$$R \text{ is the solids to gas mass flow ratio (dimensionless).}$$

The solids to gas mass flow ratio (R):

$$R = \frac{W}{\rho_g \cdot V_g} = 125.62 \tag{7.12}$$

References

[1] *Key aspects of the Paris Agreement | UNFCCC*. URL: https://unfccc.int/most-requested/key-aspects-of-the-paris-agreement (visited on 04/07/2024).

[2] jennynuss, *New UN Report: Limiting Global Warming to 1.5 Degrees Celsius Requires Deep Decarbonization Across All Sectors*, en-US, Mar. 2023. URL: https://newscenter.lbl.gov/2023/03/22/new-un-report-limiting-global-warming-requires-deep-decarbonization/ (visited on 01/07/2024).

[3] *Nuclear Fuel Fabrication - World Nuclear Association*. URL: https://world-nuclear.org/information-library/nuclear-fuel-cycle/conversion-enrichment-and-fabrication/fuel-fabrication.aspx (visited on 04/07/2024).

[4] J. Buongiorno, J. Jurewicz, M. Golay, and N. Todreas, "The Offshore Floating Nuclear Plant Concept," en, *Nuclear Technology*, vol. 194, no. 1, pp. 1–14, Apr. 2016, ISSN: 0029-5450, 1943-7471. DOI: 10.13182/NT15-49. URL: https://www.tandfonline.com/doi/full/10.13182/NT15-49 (visited on 12/18/2023).

[5] *What are Small Modular Reactors (SMRs)?* en, Text, Publisher: IAEA, Sep. 2023. URL: https://www.iaea.org/newscenter/news/what-are-small-modular-reactors-smrs (visited on 01/07/2024).

[6] D. T. Ingersoll, "2 - Small modular reactors (SMRs) for producing nuclear energy: International developments," in *Handbook of Small Modular Nuclear Reactors (Second Edition)*, ser. Woodhead Publishing Series in Energy, D. T. Ingersoll and M. D. Carelli, Eds., Woodhead Publishing, Jan. 2021, pp. 29–50, ISBN: 978-0-12-823916-2. DOI: 10.1016/B978-0-12-823916-2.00002-3. URL: https://www.sciencedirect.com/science/article/pii/B9780128239162000023 (visited on 01/07/2024).

[7] *Liquid metal cooled reactor*, en, Page Version ID: 1169470352, Aug. 2023. URL: https://en.wikipedia.org/w/index.php?title=Liquid_metal_cooled_reactor&oldid=1169470352 (visited on 01/07/2024).

[8] *Molten salt reactor*, en, Page Version ID: 1193594550, Jan. 2024. URL: https://en.wikipedia.org/w/index.php?title=Molten_salt_reactor&oldid=1193594550 (visited on 01/07/2024).

[9] J. M. Jurewicz, "Design and Construction of an Offshore Floating Nuclear Power Plant," en,

[10] J. Jurewicz, J. Buongiorno, M. Golay, N. Todreas, F. Major, and O. Skjastad, "Construction and Transportation of the Offshore Floating Nuclear Plant (OFNP)," en, 2016.

[11] R. Almeida, *Goliat FPSO Prepares for 60-Day Voyage Aboard the Dockwise Vanguard [IMAGES]*, en-US, Feb. 2015. URL: https://gcaptain.com/goliat-fpso-prepares-60-day-voyage-aboard-dockwise-vanguard-images/ (visited on 03/12/2024).

[12] *Pellet, fuel*, en-US. URL: https://www.nrc.gov/reading-rm/basic-ref/glossary/pellet-fuel.html (visited on 04/07/2024).

[13] *Fuel rod*, en-US. URL: https://www.nrc.gov/reading-rm/basic-ref/glossary/fuel-rod.html (visited on 04/07/2024).

[14] *Fuel assembly (fuel bundle, fuel element)*, en-US. URL: https://www.nrc.gov/reading-rm/basic-ref/glossary/fuel-assembly-fuel-bundle-fuel-element.html (visited on 04/07/2024).

[15] H. Nabielek and M. Mitchell, "Graphite and Ceramic Coated Particles for the HTR," en, in *Ceramic Engineering and Science Proceedings*, H.-T. Lin, A. Gyekenyesi, L. An, S. Mathur, and T. Ohji, Eds., 1st ed., vol. 31, Wiley, Sep. 2010, pp. 61–73, ISBN: 978-0-470-59474-2 978-0-470-94408-0. DOI: 10.1002/9780470944080.ch7. URL: https://ceramics.onlinelibrary.wiley.com/doi/10.1002/9780470944080.ch7 (visited on 04/07/2024).

[16] E. J. Mulder, *Mulder, e_2021_overview of x-energys 200 mwth xe-100 reactor.pdf*.

[17] *Typical prismatic fuel block (left) and a reflector block generic to... | Download Scientific Diagram*. URL: https://www.researchgate.net/figure/Typical-prismatic-fuel-block-left-and-a-reflector-block-generic-to-both-a-prismatic-and_fig9_303855627 (visited on 03/12/2024).

[18] *TRISO Particles: The Most Robust Nuclear Fuel on Earth*, en. URL: https://www.energy.gov/ne/articles/triso-particles-most-robust-nuclear-fuel-earth (visited on 04/07/2024).

[19] *Dragon Project*, en. URL: https://www.oecd-nea.org/jcms/pl_51567/dragon-project (visited on 03/13/2024).

[20] C. N. Hill, *An atomic empire: a technical history of the rise and fall of the British atomic energy programme*. London: Imperial College Press, 2013, OCLC: ocn822894618, ISBN: 978-1-908977-42-7 978-1-908977-41-0.

[21] A. A. Smith, "Decommissioning of the Dragon High Temperature Reactor (HTR) Located at the Former United Kingdom Atomic Energy Authority (UKAEA) Research Site at Winfrith - 13180," English, WM Symposia, 1628 E. Southern Avenue, Suite 9-332, Tempe, AZ 85282 (United States), Tech. Rep. INIS-US-13-WM-13180, Jul. 2013. URL: https://www.osti.gov/biblio/22224945 (visited on 03/13/2024).

[22] E. Ziermann and G. Ivens, "Final Report on the Power Operation of the AVR Experimental Nuclear Power Station.," en,

[23] R. Hecker, W. Rausch, and R. Schulten, "DEVELOPMENT OF HIGH TEMPERATURE THERMAL REACTORS IN GERMANY," en,

[24] L. L. Taylor, "Fort Saint Vrain HTGR (Th/U carbide) Fuel Characteristics for Disposal Criticality Analysis," en, Tech. Rep. DOE/SNF/REP-060, 911528, Jan. 2001, DOE/SNF/REP–060, 911 528. DOI: 10.2172/911528. URL: http://www.osti.gov/servlets/purl/911528-AYKbey/ (visited on 05/01/2024).

[25] *Fort Saint Vrain Nuclear Power Plant – Energy From Thorium*, en-US, Mar. 2023. URL: https://energyfromthorium.com/2023/03/21/ft-st-vrain-plant/ (visited on 03/13/2024).

[26] T. University, *Status report 96 - High Temperature Gas Cooled Reactor - Pebble-Bed Module.pdf*. URL: https://aris.iaea.org/PDF/HTR-PM.pdf.

[27] J. D. Werner, "U.S. Spent Nuclear Fuel Storage," en,

[28] Y. Y. Liu, "18 - Wet storage of spent nuclear fuel," in *Safe and Secure Transport and Storage of Radioactive Materials*, K. B. Sorenson, Ed., Oxford: Woodhead Publishing, Jan. 2015, pp. 299–310, ISBN: 978-1-78242-309-6. DOI: 10.1016/B978-1-78242-309-6.00018-6. URL: https://www.sciencedirect.com/science/article/pii/B9781782423096000186 (visited on 03/12/2024).

[29] *Dry Cask Storage and Transportation*, en-US. URL: https://holtecinternational.com/products-and-services/nuclear-fuel-and-waste-management/dry-cask-and-storage-transport/ (visited on 03/12/2024).

[30] N. P. Ventikos and D. I. Stavrou, "Ship to Ship (STS) Transfer f Cargo: Latest Developments and Operational Risk Assessment," en, vol. 63, no. 3, 2013.

[31] KaranC, *What are Very Large Crude Carrier (VLCC) and Ultra Large Crude Carrier (ULCC)?* en-US, Jan. 2023. URL: https://www.marineinsight.com/types-of-ships/what-are-very-large-crude-carrier-vlcc-and-ultra-large-crude-carrier-ulcc/ (visited on 03/28/2024).

[32] T. Tokić, V. Frančić, N. Hasanspahić, and I. Rudan, "Training Requirements for LNG Ship-to-Ship Transfer," en, *Journal of Maritime & Transportation Science*, vol. 60, no. 1, pp. 49–63, Jul. 2021, ISSN: 1848-9052, 0554-6397. DOI: 10.18048/2021.60.03. URL: https://hrcak.srce.hr/clanak/379606 (visited on 03/28/2024).

[33] E. A. Tannuri, J. C. Pereira, F. Ruggeri, R. S. Lavieri, F. Rateiro, A. S. S. Ianagui, F. Haranaka, and R. Watai, "Anchored Vessel Ship-to-Ship Operations: Environmental Limits Considering Mooring Equipments and Ship Maneuver," en, *SSRN Electronic Journal*, 2016, ISSN: 1556-5068. DOI: 10.2139/ssrn.3550698. URL: https://www.ssrn.com/abstract=3550698 (visited on 03/28/2024).

[34] Murdjito, M. P. Rosari, and E. B. Djatmiko, "Analysis on the Critical Conditions of Side-by-Side Offloading Operation between SSP Type-FPSO and Shuttle Tanker," en, *Applied Mechanics and Materials*, vol. 874, pp. 53–63, Jan. 2018, ISSN: 1662-7482. DOI: 10.4028/www.scientific.net/AMM.874.53. URL: https://www.scientific.net/AMM.874.53 (visited on 03/28/2024).

[35] F. Hopen, *Cylindrical FLNG Technology & cost savings for Cylindrical FLNG vs Ship Shaped FLNG.pdf*.

[36] Z. Zhang, Z. Wu, D. Wang, Y. Xu, Y. Sun, F. Li, and Y. Dong, "Current status and technical description of Chinese 2×250MWth HTR-PM demonstration plant," en, *Nuclear Engineering and Design*, vol. 239, no. 7, pp. 1212–1219, Jul. 2009, ISSN: 00295493. DOI: 10.1016/j.nucengdes.2009.02.023. URL: https://linkinghub.elsevier.com/retrieve/pii/S0029549309001332 (visited on 12/18/2023).

[37] H. Liu, D. Du, Z. Han, Y. Zou, and J. Pan, "Dynamic analysis and application of fuel elements pneumatic transportation in a pebble bed reactor," en, *Energy*, vol. 79, pp. 33–39, Jan. 2015, ISSN: 03605442. DOI: 10.1016/j.energy.2014.09.021. URL: https://linkinghub.elsevier.com/retrieve/pii/S0360544214010779 (visited on 04/21/2024).

[38] *Mitsubishi Power | M501G Series*, en. URL: https://power.mhi.com/products/gasturbines/lineup/m501g (visited on 03/16/2024).

[39] K. Singh, *GI-Overview of HI-STAR Technology*. URL: 1997.

[40] J. Wang, B. Wang, B. Wu, and Y. Li, "Design of the Spent Fuel Storage Well of HTR-PM," en, in *Volume 1: Operations and Maintenance, Aging Management and Plant Upgrades; Nuclear Fuel, Fuel Cycle, Reactor Physics and Transport Theory; Plant Systems, Structures, Components and Materials; I&C, Digital Controls, and Influence of Human Factors*, Charlotte, North Carolina, USA: American Society of Mechanical Engineers, Jun. 2016, V001T03A003, ISBN: 978-0-7918-5001-5. DOI: 10.1115/ICONE24-60051. URL: https://asmedigitalcollection.asme.org/ICONE/proceedings/ICONE24/50015/Charlotte,%20North%20Carolina,%20USA/251531 (visited on 12/18/2023).

[41] *HI-STAR*, en-US. URL: https://holtecinternational.com/products-and-services/nuclear-fuel-and-waste-management/dry-cask-and-storage-transport/hi-star/ (visited on 05/01/2024).

[42] J. Wang, Z. Zhang, B. Wu, and Y. Li, *DESIGN OF THE HTR-PM SPENT FUEL STORAGE FACILITY.pdf*.

[43] *Decay heat*, en, Page Version ID: 1219490611, Apr. 2024. URL: https://en.wikipedia.org/w/index.php?title=Decay_heat&oldid=1219490611 (visited on 04/18/2024).

[44] *Lamson 2400 | High Flow Multistage Centrifugal Blower | Hoffman & Lamson*, en-US. URL: https://www.hoffmanandlamson.com/en-us/products/centrifugal-blowers-exhausters/multistage-centrifugal/high-flow-multistage-centrifugal-blowers/lamson-2400 (visited on 04/14/2024).

[45] *First Law of Thermodynamics Summary*. URL: https://webhome.phy.duke.edu/~rgb/Class/phy51/phy51/node59.html (visited on 04/18/2024).

[46] *Largest module in place at second Vogtle AP1000 - World Nuclear News*. URL: https://www.world-nuclear-news.org/Articles/Largest-module-in-place-at-second-Vogtle-AP1000 (visited on 04/15/2024).

[47] *Cask handling cranes | Konecranes USA*, en-us. URL: https://www.konecranes.com/en-us/industries/nuclear/nuclear-equipment/cask-handling-cranes (visited on 05/02/2024).

[48] J. G. Liu, H. L. Xiao, and C. P. Li, "Design and full scale test of the fuel handling system," en, *Nuclear Engineering and Design*, 2002.

[49] R. Springman, *Holtec International: Multi-Purpose Canisters for Long-Term Interim Storage*, Jun. 2015. URL: https://www-pub.iaea.org/iaeameetings/cn226p/Session5/ID147Springman.pdf (visited on 05/01/2024).

[50] B. Wu, J. Wang, Y. Li, H. Wang, and T. Ma, "Design, Experiment, and Commissioning of the Spent Fuel Conveying and Loading System of HTR-PM," en, *Science and Technology of Nuclear Installations*, vol. 2022, A. Serikov, Ed., pp. 1–8, Apr. 2022, ISSN: 1687-6083, 1687-6075. DOI: 10.1155/2022/1817191. URL: https://www.hindawi.com/journals/stni/2022/1817191/ (visited on 12/18/2023).

[51] U. D. of Energy, *Vertical-Cask-Transporter.pdf*. URL: https://www.chbwv.com/graphics/Vertical-Cask-Transporter.pdf (visited on 03/17/2024).

[52] MacGregor, *MacGregor-Crane-Technical-Specifications.pdf*.

[53] G. Swinglink, "Bucket Material," en, URL: https://www.goughecon.com/wp-content/uploads/2018/12/bucketflyeredit2.pdf.

[54] *Swinglink™ - Industrial Conveyors And Bucket Elevators*, en-US. URL: https://www.goughecon.com/product-details/swinglink-industrial-conveyors-elevators (visited on 05/02/2024).

[55] G. Swinglink, *Swinglink® Heavy Duty Bucket Elevators*. URL: https://www.goughecon.com/wp-content/uploads/2018/12/swinglinkind.pdf (visited on 03/29/2024).

[56] *Stainless Steel Grade 303 / 1.4305 Material Properties*. URL: https://www.farnell.com/datasheets/26031.pdf (visited on 03/29/2024).

[57] S. Sakakibara and S. Yamada, "Fender Selection for Reverse Lightering of Ship-to-Ship Transfer Operations," en, in *Volume 1: Offshore Technology*, Estoril, Portugal: ASMEDC, Jan. 2008, pp. 645–654, ISBN: 978-0-7918-4818-0. DOI: 10.1115/OMAE2008-57589. URL: https://asmedigitalcollection.asme.org/OMAE/proceedings/OMAE2008/48180/645/328554 (visited on 03/28/2024).

[58] *Yokohama Pneumatic Fender - Rubber Fender | YSmarines*, en-US, Section: Rubber Fender, Jul. 2022. URL: https://www.ysmarines.com/rubber-fender/yokohama-pneumatic-rubber-fender/ (visited on 03/28/2024).

[59] *Brasil Knutsen*. URL: https://knutsenoas.com/ship/brasil-knutsen/ (visited on 04/16/2024).

[60] N. Burdine, "Design of a pneumatic conveying test loop for laboratory testing," en,

[61] *Modular Gangways | Tyne Gangway*, en-GB, Sep. 2018. URL: https://www.tynegangway.com/product/modular-gangways/ (visited on 03/30/2024).

[62] *Lead Price*. URL: https://www.dailymetalprice.com/lead.html (visited on 04/11/2024).

[63] S.-i. Tanaka and T. Suzuki, "A calculational method of photon dose equivalent based on the revised technical standards of radiological protection law," en, Tech. Rep. ORNL/TR-90/29, 6197219, Mar. 1991, ORNL/TR–90/29, 6 197 219. DOI: 10.2172/6197219. URL: http://www.osti.gov/servlets/purl/6197219/ (visited on 04/09/2024).

[64] *Concrete Calculator - How Much Concrete Do I Need? - Concrete Network*, en. URL: https://www.concretenetwork.com/concrete/howmuch/calculator.htm (visited on 04/11/2024).

[65] *Hosecraft USA : Quality SB1 Stainless Steel Corrugated Braided Metal Hose*. URL: https://www.hosecraftusa.com/model/SB1_Stainless_Single_Braided_Metal_Hose (visited on 04/09/2024).

[66] A. Bahtia, *Pneumatic Conveying Systems.pdf*. URL: https://www.cedengineering.com/userfiles/M05-010%20-%20Pneumatic%20Conveying%20Systems%20-%20US.pdf.

[67] *Volumetric flow rate*, en, Page Version ID: 1194938479, Jan. 2024. URL: https://en.wikipedia.org/w/index.php?title=Volumetric_flow_rate&oldid=1194938479 (visited on 04/19/2024).

[68] *DRIVING CENTRIFUGAL COMPRESSOR TECHNOLOGY*. URL: https://www.atlascopco.com/content/dam/atlas-copco/compressor-technique/gas-and-process/documents/driving-centrifugal-compressor-technology.pdf.

[69] *TurboBlock (TM) standardized centrifugal compressor*, en-US. URL: https://www.atlascopco.com/en-us/compressors/products/processairgasequipment/centrifugal-compressors/turbo-block-compressor (visited on 04/02/2024).

[70] *Dropsafe Custom Solutions*, en-GB. URL: https://dropsafe.com/product/custom-solutions (visited on 03/31/2024).

[71] *Potential and Kinetic Energy*. URL: https://www.mathsisfun.com/physics/energy-potential-kinetic.html (visited on 04/19/2024).

[72] *Steel Nets | Shop Stainless Steel Netting & Custom Metal Nets Online*, en. URL: https://www.usnetting.com/safety-netting/steel-netting/ (visited on 04/10/2024).

[73] *Top 10 Deepest Sea Ports in the World*, en-US, Section: UPSC, Mar. 2024. URL: https://www.geeksforgeeks.org/top-10-deepest-sea-ports-in-the-world/ (visited on 03/29/2024).

[74] *MARINE SAFETY INFORMATION BULLETIN (MSIB) 2-17: LIGHTERING AND SHIP TO SHIP TRANSFER OPERATIONS*. URL: https://homeport.uscg.mil/Lists/Content/Attachments/1537/02-17%20-%20Lightering%20and%20Ship%20to%20Ship%20Transfer%20Operations.pdf (visited on 05/03/2024).

[75] *Beam Deflection Tables | MechaniCalc*. URL: https://mechanicalc.com/reference/beam-deflection-tables (visited on 04/12/2024).

[76] *High Flow Multistage Centrifugal Blowers | Hoffman & Lamson*, en-US. URL: https://www.hoffmanandlamson.com/en-us/products/centrifugal-blowers-exhausters/multistage-centrifugal/high-flow-multistage-centrifugal-blowers (visited on 03/17/2024).

[77] *Duplex 2507 Stainless Steel*, en-US. URL: https://www.pennstainless.com/resources/product-information/stainless-grades/duplex-grades/duplex-2507-stainless-steel/ (visited on 03/30/2024).

[78] S. Fang, J. Cao, W. Li, C. Luo, F. Yao, X. Li, and K. Li, "Shielding Design and Dose Evaluation for HTR-PM Fuel Transport Pipelines by QAD-CGA Program," en, *Science and Technology of Nuclear Installations*, vol. 2021, K. E. Holbert, Ed., pp. 1–6, May 2021, ISSN: 1687-6083, 1687-6075. DOI: 10.1155/2021/6686919. URL: https://www.hindawi.com/journals/stni/2021/6686919/ (visited on 04/07/2024).

[79] *0481 - H201 - Health Physics Technology - 05 - Shielding - Gamma Constant - Point Source/Inverse Square - Line Source, Area Source & Volume Source.* URL: https://www.nrc.gov/docs/ML1126/ML11262A163.pdf (visited on 04/15/2024).

[80] *Lecture 6-Radiation Shielding | PPT*. URL: https://www.slideshare.net/erletshaqe1/lecture-6-30005233 (visited on 04/09/2024).

[81] B. Buyuk, "Gamma Attenuation Behavior of Some Stainless and Boron Steels," en, *Acta Physica Polonica A*, vol. 127, no. 4, pp. 1342–1345, Apr. 2015, ISSN: 0587-4246, 1898-794X. DOI: 10.12693/APhysPolA.127.1342. URL: http://przyrbwn.icm.edu.pl/APP/PDF/127/a127z4p132.pdf (visited on 04/12/2024).

[82] B. Lauridsen, "Table of Exposure Rate Constants and Dose Equivalent Rate Constants," en, URL: https://backend.orbit.dtu.dk/ws/portalfiles/portal/56550773/ris_m_2322.pdf.